ELSEVIER

Coordination Chemistry Reviews
214 (2001) 143–185

COORDINATION CHEMISTRY REVIEWS

www.elsevier.com/locate/ccr

Revisiting the main group cyclopentadienyl metal complexes in terms of the through-space coupling concept

Valentin N. Sapunov [b], Karl Kirchner [a], Roland Schmid [a,*]

[a] *Institute of Inorganic Chemistry, Technical University of Vienna, Getreidemarkt 9/153, A-1060 Vienna, Austria*
[b] *D. Mendeleev University of Chemistry and Technology of Russia, Miusskaja 9, 125190 Moscow, Russia*

Received 31 May 2000; accepted 25 September 2000

Contents

Abstract . . . 144
1. Introduction . . . 144
1.1. Bonding in main group Cp′ complexes . . . 146
1.2. The through-space-coupling (TSC) concept . . . 147
1.3. Cation-π interactions . . . 148
2. s^0p^0 metal systems . . . 150
2.1. Half-sandwich complexes . . . 150
2.2. Metallocenes . . . 156
2.2.1. Planar systems . . . 156
2.2.2. Distortions . . . 159
2.2.2.1. Slippage . . . 160
2.2.2.2. Bending . . . 160
2.3. Tris(Cp) complexes . . . 167
3. s^2p^0 metal systems . . . 170
3.1. Half-sandwich complexes . . . 170
3.1.1. σ donor properties . . . 171
3.1.2. σ acceptor properties . . . 173
3.2. s^2p^0 metallocenes . . . 174
3.2.1. Acceptor properties . . . 177
3.3. Tris(Cp) complexes . . . 178
4. Summary and outlook . . . 180
References . . . 181

* Corresponding author. Fax: +43-1-5880115399.
E-mail addresses: vals@muctr.edu.ru (V.N. Sapunov), rschmid@mail.zserv.tuwien.ac.at (R. Schmid).

0010-8545/01/$ - see front matter © 2001 Elsevier Science B.V. All rights reserved.
PII: S0010-8545(00)00390-8

Abstract

The structures and properties of metal complexes are traditionally treated in terms of hybridization and electronic ligand effects. What is notoriously neglected, however, is the fact that in such an aggregate the ligands approach so closely to one another — on the order of van der Waals (vdW) distances — that intramolecular packing effects come into play. Actually, non-bonded interactions between any atoms bonded to some central atom are increasingly recognized as an important factor in determining bond distances, bond angles and the like. The class of the main group cyclopentadienyl (Cp) metal complexes appears to be a case study in this respect, because of the large extension of the Cp group and its ring structure on the one hand, and on the other, the minimal d-orbital involvement, dissimilar to the transition-metal analogues. It is shown that the diverse array of structural arrangements, such as linear, ring-slipped, bent, and polymeric chain structures, as well as their reactivities, are brought under the umbrella of one treatment with the aid of the through-space coupling (TSC) concept. This is the molecular orbital representation of vdW repulsive–attractive forces. As a central feature, the individual ligands are at first combined to a united system of TSC orbitals and then allowed to interact with the metal AOs. The energy splitting of the TSC orbitals and the electron density shift from one of them to a vacant metal orbital determine the repulsive and attractive interligand forces and hence fine-tune the geometry of the complex. Along these lines a physical explanation for the interplay between vdW attraction and repulsion becomes available. More specifically we are dealing here with complexes of the type Cp'_nML_m ($n = 1–3$, $m = 0–3$) via united $\{Cp'_nL_m\}$ molecular orbitals. Bending and slipping of the Cp′ ligands are rooted in vdW attraction and repulsion, respectively, with geometry and hapticity of the Cp′-metal bonding adjusted so as to optimize TSC. © 2001 Elsevier Science B.V. All rights reserved.

Keywords: Bond theory; Coordination chemistry; Cyclopentadienes; Main group elements; Through-space interactions

1. Introduction

The considerable importance of the cyclopentadienyl anion ($[C_6H_5]^-$, Cp) as a ubiquitous ligand is obvious from the fact alone that this entity has been admitted to the common keyword catalogue. In addition, there are a large number of substituted varieties, above all these is the pentamethyl derivative Cp*. Thus, Cp′ is used as a general abbreviation for Cp and derivatives of Cp. More specifically, cyclopentadienyl metal complexes of the types $Cp'ML_n$ and Cp'_2ML_m are of widespread interest for their relevance in catalytic [1–3] and stoichiometric [4–7] organic syntheses. In these transformations, the Cp′ fragment typically acts as a 'spectator' ligand, because of the multiple, hence strong, bonding relative to the co-ligands. Molecular orbital (MO) studies performed by several authors have shed some light on how the filling and mixing of s–p or s–p–d orbitals of the metal relate to both geometry and donor–acceptor properties of the $Cp'ML_n$ complexes [8–17].

From the structural and bonding patterns it is convenient to separate the Cp′ complexes into transition metal and main group compounds. Of these, the d metal complexes are best understood because of the key role played by the metal d orbitals in the π interactions with the ring. The importance of covalence in these species and of the involvement of the metal d orbitals is stressed by the rigid electronic requirements of simple metallocenes conforming to the 18-electron rule.

The main group counterparts differ markedly in at least two respects. Firstly, they exhibit a broad range of ring-coordination geometries, such as ring-slipped, bent, and polymeric chain structures, and reactivities. Furthermore, these chameleon-like features are highly fluctional and are highly sensitive to the nature of the other ligands as well as the substitution of the Cp′ ring [18,19]. Secondly, there is no adherence to simple formal electron counting rules, either to the eight-electron rule (d orbitals not participating) or to the 18-electron rule (d orbitals participating). So-called 'islands of electronic stability' of the eight-, 14- and 20-electron constructions are empirical rules with many exceptions (e.g. CpSnCl, ten electrons; Cp_2Mg, 12 electrons) [16,20]. These rules, with the '$4n + 2$ interstitial electron rule' [21] and the '14 interstitial electron rule' [22] as forerunners, still await a theoretical explanation, however.

The great structural variety observed and the less restricted electronic requirements are commonly rationalized in terms of minimal d orbital involvement and the more varied (ionic and/or covalent) character of the metal–ligand interactions, although the extent of ionic character is still vague. Particularly the Group 1 metal compounds are thought to be highly ionic implying that the cation spheres collect as many anions and dipolar ligand molecules in their coordination spheres as possible, only defined by steric limits [23]. The diverse array of structural arrangements has been comprehensively reviewed by Jutzi [24] and Jutzi and Burford [25]. Also, the review on the Cp′-alkali metal chemistry by Harder [23] and that on p-block metallocenes by Beswick et al. [16] should be mentioned. A major conclusion to be drawn from these papers, in connection with many others, is that main group complex structures in general cannot be explained satisfactorily without implication of non-bonded ligand–ligand interactions, in other words, intramolecular packing effects [26]. The final structure would ultimately depend on a delicate balance between ionicity, π bonding and non-bonded interactions.

Although traditional approaches have generally ignored the size and shape of coordinated ligands, the importance of non-bonded interactions between any atoms bonded to some central atom is increasingly recognized as an important factor determining bond distances, bond angles and the like. Such a relationship has recently been discussed with fluorine compounds [27]. First impulses in this direction go back to Pitzer [28] and Bartell [29] who claimed that non-bonded interactions in molecules are even more relevant than effects of hybridization and conjugation. Due to the size and the shape of the Cp′ group, non-bonded effects are particularly obvious in the title metal complexes, which therefore appear to be a case study in this respect.

1.1. Bonding in main group Cp′ complexes

According to the three interaction modes — ionic, covalent and non-bonded — three models have been suggested to describe the structure of main group cyclopentadienyl metal complexes [30], in particular to answer the question when metallocenes are bent (i.e. non-parallel ring orientations): (i) an orbital overlap or mixing model involving d orbitals [31,32]; (ii) an electrostatic (polarized-ion) model [33]; and (iii) a model based on inter-ligand van der Waals (vdW) repulsive–attractive forces [26,34]. The orbital overlap model may be adequate for the transition metal complexes where a connection could exist between the degree of bending and the d orbital occupancy, but failed to identify bent geometries as energy minima for main group compounds [35]. The problem rests in the ambiguous effects of electronic and steric factors. The electrostatic model is based on the polarization argument used to analyze bent vs. linear MX_2 gaseous alkaline earth metal dihalides [36]. Accordingly, polarization of the cation by one Cp anion could diminish the electrostatic interaction between the cation and the second Cp′ anion directly opposite, thus favoring a bent geometry [37].

From the above, the model based on size considerations appears to be the most intriguing. In fact, a rough subdivision of the main group metallocenes into planar (linear), bent and slipped structures is available by simple size arguments as follows. In virtually all linear varieties, the interplanar distances between the planes of the Cp′ ligands are found in the range 3.7–4.7 Å, i.e. a M–Cp plane distance between 1.8 and 2.3 Å. Bending sets in at larger distances than this [26]. On the other hand, in the slipped sandwich structures the M–Cp′ plane distances are shorter by about 1.8 Å [23]. Thus, the criterion for distinguishing between slipped and bent sandwich structures is a M–Cp plane distance close to the vdW radius of 1.77 Å for aromatic carbon [38].

In this frame, the reason for slipped sandwich structures is avoidance of unfavorable repulsions between the Cp′ rings. In the bent structures, similarly, the degree of bending is limited by the repulsions between the planes' borders [26]. The experimental value of the shortest methyl group carbon–carbon distance of the Cp* ligands is found [39,40] at about 4.1 Å, close to twice the methyl vdW radius (2.0 Å) [41].

In this context the interlayer distance in graphite, being 3.35 Å, should be mentioned, would project a carbon vdW radius smaller than 1.77 Å. As a matter of fact, however, every layer in graphite is shifted half a ring over, actually paralleling ring slippage in metallocenes. A similar phenomenon occurs with polynuclear hydrocarbons such as 1,2:7,8-dibenzocoronene ($C_{32}H_{16}$) exhibiting a perpendicular distance of 3.45 Å between the aromatic planes [42]. Finally, while slipping is rooted in vdW repulsion, bending in turn should be due to interligand vdW attraction as will be shown below. Unfortunately, a definite physical explanation for the interplay between vdW attraction and repulsion is still elusive.

It should be emphasized that both the above models (polarized ion (ii) and vdW (iii)) could also be couched in molecular orbital terms. For (ii), an ion is polarizable to the extent that it has low-lying vacant orbitals. The interaction of Cp′ anions

with a polarizable metal center is equivalent to interaction with these vacant orbitals [33]. For (iii), vdW repulsive–attractive forces virtually correspond to through-space coupling (TSC), with the terminology coined by Hoffmann [43–47].

1.2. The through-space-coupling (TSC) concept

The basic idea is that in a metal complex the ligands approach so close to one another that filled–filled interactions come into play. When two localized orbitals (vacant or filled) interact, two new orbitals, combined by sum and difference, are formed, a lower energy symmetric (in-phase) form Ψ_s^{TSC} and a higher energy anti-symmetric (out-of-phase) form Ψ_a^{TSC}. The energy splitting between the two orbitals is a quantitative measure of orbital interaction. If both orbitals are doubly occupied, there is indeed an overall loss in energy corresponding to vdW repulsion. If, on the other hand, electron density is removed from one of the TSC orbitals into some vacant orbital, the molecular construction is stabilized corresponding to vdW attraction. This happens, e.g. in the aromatic radical systems 1,3,2-dithiazol-2-yl [48] and 1,3,5-trithia-2,4,6-triazapentalenyl [49]. In the crystalline state, the almost planar molecules form loose dimers placed in quasi-parallel stacks with intermolecular S–S distances of 3.14 and 3.18 Å (in the order quoted above). These are shorter than twice the vdW radius of S (3.7 Å) and actually reflect the operation of vdW attractive forces. Similar π-through-space interactions with aromatic co-ligands may be the origin of the phenomenon known as the 'aromatic ring current effect' [50] or 'ring stacking interaction' [51].

The possibility of such charge redistributions imply that the so-called vdW radius, allegedly determined by the balance of attractive and repulsive forces between valence-saturated non-bonded atoms, is not a constant, but can vary with the nature of the partner. This appears to be the root of the discrepancies between the vdW radii and the so-called non-bonded radii, with the latter defined as 'the distance at which bonding and non-bonded forces cancel' [52]. From a theoretical point of view, however, vdW and non-bonded radii should be basically equivalent. In solid molecular chlorine, for instance, the short nearest-neighbor contact of 3.28 Å is significantly less than twice the commonly accepted vdW radius of 1.80 Å [53]. As the authors realized, the layered crystal structure found is indicative of a specific directed intermolecular interaction involving charge transfer due to Lewis acid and Lewis base sites within the valence shell of the constituent atoms. The above-mentioned variability of the vdW radius of carbon may be explained in similar terms.

Here we are concerned with Cp′ metal complexes of Groups 1, 2, 13, 14 and 15 of the types Cp'_nML_m ($n = 1–3$, $m = 0–3$). In the TSC picture, the n Cp′ and m L ligands are considered as a united system of mutual TSC orbitals which can act as σ donor (in general from Ψ_s^{TSC}) or as a π donor (in general from Ψ_a^{TSC}). The electronic and geometric structure of the Cp'_nML_m complex is derived from the interaction between the metal AOs and the mutual TSC orbitals of the $\{Cp'_nL_m\}$ system. The energy splitting of the TSC orbitals and the electron density shift from them to vacant metal orbitals determine the repulsive and attractive interligand forces and hence fine-tune the stability of the complex. Both geometry and hapticity of the Cp′–metal bonding are adjusted so as to optimize the TSC.

The aim of this article is to show that by a simple TSC picture the large diversity in molecular shapes and reactivities of the main group metal Cp complexes can be brought under the umbrella of one treatment. Along these lines we advocate the relevance of covalent (i.e. directional, irrespective of charge transfer) interactions to the structure even of the Group 1 Cp–M complexes. Even if the bonding in this group of compounds is almost ionic in nature, orbital overlap arguably is the decisive factor determining the structural peculiarities.

It may be emphasized that our concept of vdW repulsions conforms well with that advanced many decades ago by Mulliken, namely that such non-bonded repulsions are a manifestation of covalent anti-bonding. On the other hand, what we call vdW attractions differ appreciably from the historic usage according to which such attractions are a consequence of the electron correlation associated with London dispersion forces. Such forces are totally absent in the results of HF, SCF and MO calculations.

1.3. Cation-π interactions

From electronegativity considerations, of course, the Cp–M bond is the more ionic the more the metal is electropositive. There have been many efforts to evaluate the covalent and ionic contributions to the bonding in these complexes, but final results are elusive [23]. For instance, Sockwell and Hanusa analyzed the plots of the metal–Cp distances in a large number of Cp complexes versus the (ionic) metal radii. While, in the ionic limit, additivity of radii requires that such plots have a slope of unity, this is not the case, even for the divalent complexes [54].

Fortunately, for bonding considerations, the distinction between the two traditional approaches of covalency and ionicity is becoming increasingly less meaningful in the light of the complete parallelism between ionic and covalent bonds [55]. More specifically, and unexpectedly from classical theories, there is a relatively strong interplay between an aromatic and even alkali metal ions, with the gas-phase binding energies being very sensitive to the cation size. Note that the energy between K^+ and benzene at -77 kJ mol^{-1} is even slightly greater than that of K^+ and water at -75 kJ mol^{-1} [56,57]. Similarly, the interactions of benzene with Li^+, BeH^+ and LiH have been calculated by ab initio SCF and MO theory to be quite exothermic, viz. -353, -193, -572 kJ mol^{-1}, respectively [21]. Even between atomic lithium and benzene a significant electronic interaction takes place as judged from IR spectra of the neutral unstable complexes BzLi and Bz_2Li, characterized by a normal coordinate analysis as interactions between the Li $2p_x$ and $2p_y$ AOs and the benzene π-system [58].

The interplay between the π-electron cloud of an aromatic (or any other π system such as alkenes) with a cation is called cation–π interaction [57]. It may be classified as non-covalent since it is primarily electrostatic in nature, with the ion–quadrupole interaction accounting for 60% of the binding energy. However, this interaction may also be interpreted as non-ionic since the resulting bonding is directional. Note for instance the multihapto interaction mode exhibited between Cs and the aryl ring carbon atoms in the crown ether adducts of CsP(H)R

(R = 2,4,6-tri-*tert*-butylphenyl and 2,6-dimesitylphenyl) [59]. Finally, for the less electropositive metal ions the interactions are increasingly covalent such as in cationic $[Cp_2Al]^+$ [60] or neutral Cp^*_2Ge [11] with, nevertheless, minor or absent d orbital contribution.

It is useful to distinguish two types of π interactions, viz. axial and non-axial, between the metal and the Cp ring with the relative contributions depending on the electronic configuration of the complex. The electronic construction is largely determined by the interaction between the Cp′ π system $\{\pi_{sym}\ (a_2'')$ and two $\pi_{asym}\ (e_1'')\}$ and the {s, p} metal set. According to Fig. 1, the a_2'' orbital of Cp interacts strongly with the metal s and p_z AOs forming three centrosymmetric MOs: the bonding $1a_1$ orbital ($\langle s \mid a_2'' \rangle$ and $\langle p_z \mid a_2'' \rangle$ or, as an approximation, $\langle s,p_z \mid a_2'' \rangle$), the $2a_1$ orbital (classical metal sp, and practically non-bonding), and the high-lying anti-bonding $3a_1$ orbital (as a result of the $\langle s,p_z \mid a_2'' \rangle$ interaction). The $\langle s,p_z \mid a_2'' \rangle$ interaction is responsible for the commonly found perfect η^5 hapticity of the centered-ring metal bonding. When, for LiCp, Li^+ is moved in steps above the Cp ring, calculations show that both the energy and the Cp(plane)–Li distance increase with decreasing hapticity [23].

The two other filled Cp′ π orbitals ($e_1'' \equiv \pi_{asym}$) overlap (rather weakly, relative to $\langle \pi_{sym} \mid sp \rangle$) with the degenerate p_y and p_x metal AOs. As a result of the $\langle p_x \mid e_1'' \rangle$ and $\langle p_y \mid e_1'' \rangle$ interactions (Fig. 2), two bonding (occupied, $1e_1$) and two anti-bonding ($2e_1$) orbitals both of δ symmetry are formed [10,61]. The occupied bonding molecular orbitals ($1a_1$ Fig. 1) and two $1e_1$ orbitals (Fig. 2) have considerably more ligand character (practically the π_{sym} and π_{asym} MOs of Cp), whereas the non-bond-

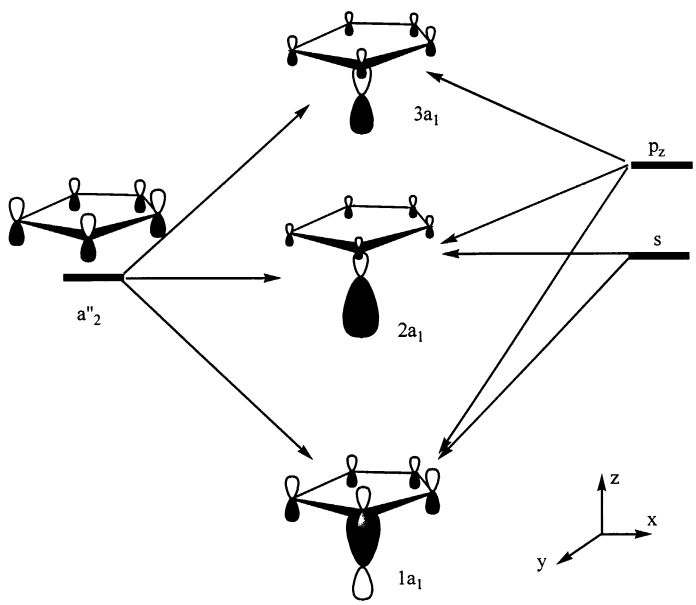

Fig. 1. The interaction of a_2'' of Cp with the s and p_z metal AOs.

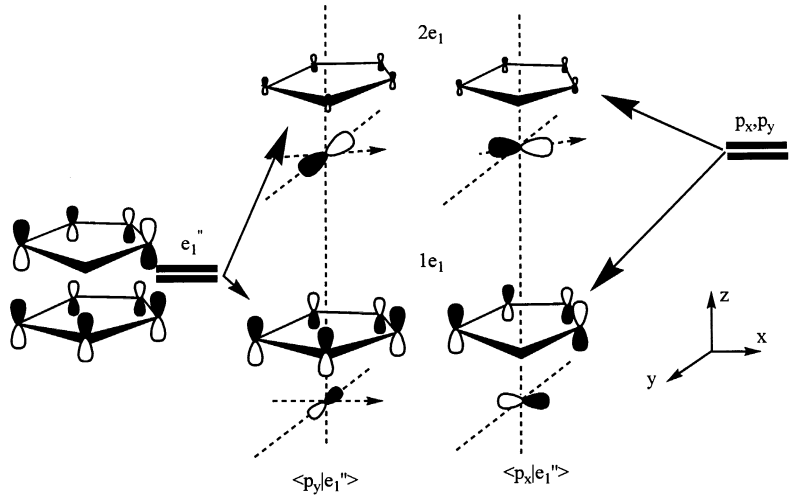

Fig. 2. The interaction of e''_1 of Cp with the p_x and p_y metal AOs.

ing ($2a_1$) and the anti-bonding ($2e_1$) MOs have more metal-like character (practically sp_z and p_x, p_y). The axial $\langle s,p_z \mid a_2'' \rangle$ interaction determines the construction of the complex and is realized by the shift in electron density from a_2'' of Cp into the metal s and p_z. Although the non-axial interaction of the π_{asym} MOs of Cp with the metal p_y and p_x AOs contributes little to the Cp-metal stability (small overlap), it virtually controls the hapticity of the Cp–M bond and the amount of electron density taken over from the Cp ligand. The energy of the shift η^5-Cp–M $\rightarrow \eta^1$-Cp–M costs 82 kJ mol^{-1} for Li and 43.5 kJ mol^{-1} for Na [62].

In view of the Cp π system being a donor to both the metal s and p AOs and the potentially high s/p energy gap, i.e. high costs of s/p mixing, it is appropriate to differentiate between the two cases of empty and filled metal s AO, i.e. s^0p^0 and s^2p^0 metal systems. Note that all sketches to follow are qualitative ones, i.e. they indicate the correct symmetry but not a very faithful idea of the correct relative contributions around the Cp ring.

2. s^0p^0 metal systems

2.1. Half-sandwich complexes

In the Cp′M complexes of monovalent alkali, divalent alkaline earth and trivalent Group 13 metals, without sp_z and p_x, p_y mixing, all three π-orbitals of Cp′ and the metal {s, p} set are involved. Consequently, the η^5 bonding mode is stable. With the low-lying non-bonding (sp) orbital empty, the Cp′M fragment is coordinatively unsaturated and is both a σ and a π acceptor (Fig. 3).

With monodentate σ donors, the Cp′M fragment forms C_{5v} symmetric adducts such as $[Cp^*BBr]^+$ [63], $[Cp^*BI]^+$ [64], $CpCu(PPh_3)$ [65], CpBeCl [66], and $(Ph_5C_5)Cu(PPh_3)$ [67]. (The adducts of Refs. [65,67] cannot, of course, correspond to strictly C_{5v} symmetry.) It is noteworthy that the completely filled d orbitals in the copper complexes do not disturb the 'pogo-stick' complex construction. Ab inito calculations show that the eight-electron complex [CpBeH] strongly prefers C_{5v} symmetry with highly covalent η^5 bonding [68]. Evidence of the C_{5v} symmetry stems from the microwave spectra of CpBeH, CpBeD, $^{13}CC_4H_5BeH$ and $^{13}CC_4H_5BeD$ [69]. This structure is preserved even in the presence of bulky substituents on the Cp ring as in the adduct of tris(trimethylsilyl) cyclopentadienyl-lithium with quinuclidine [70]. Weak σ-donor ligands yield weak complexes as found between CpNa and H_2O giving $CpNa(H_2O)$ with a bonding energy of 63.6 kJ mol^{-1} [62].

Furthermore, the two π acceptor orbitals ($2e_1$) of Cp′M can interact face-to-face with suitable p and/or π ligand orbitals, but in contrast to the rather strong axial σ-interaction, this π interaction is weak, because of its anti-bonding character. In fact, ab initio calculations of $CpNa(CH_2{=}CH_2)$ point to small bonding energies (33 kJ mol^{-1}) between CpNa and $CH_2{=}CH_2$ [62]. Therefore, if the apex σ ligand has additional *n*p orbitals such as in [:C≡CR], Cl^- or Br^-, the M–L bonding energy is not much affected by the π interaction. This is reflected by the small Jahn–Teller splitting of the order of 0.1–0.2 eV as derived from He(I) photoelectron spectra of CpBeX, where X are the above ligands [71].

Much stronger interactions occur in the $Cp'ML_n$ ($n > 1$) complexes between the σ and π acceptor orbitals of the CpM unit and the L_n ligands, forming two, three (piano stool) or even four legged structures such as Cp′Li(tmeda) (Cp′ = $C_5H_4SiMe_3$, tmeda = $Me_2NCH_2CH_2NMe_2$) [72], $Cp^*Na(Py)_3$ [73], $Bz_5C_5K(thf)_3$ [74], CpLi(12-crown-4) [75] or the row $CpLi(NH_3)$, $CpLi(NH_3)_2$, $CpLi(NH_3)_3$ [76]. The competition between the anionic Cp^- and the group of coligands for metal orbitals leads to the destabilization of the Cp-M bond and is seen by an increase in the Cp-metal distances [77,78]. SCF calculations suggest that stepwise NH_3 coordi-

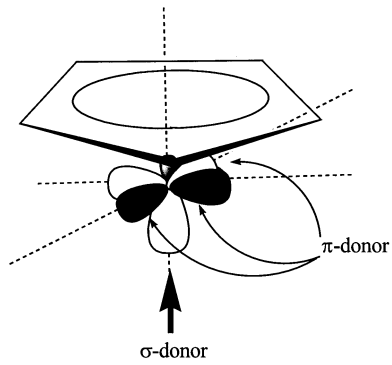

Fig. 3. The interaction of the $2a_1$ and $2e_1$ orbitals with a σ- and/or π-donor ligand.

nation in the series $CpLi \rightarrow CpLi(NH_3) \rightarrow CpLi(NH_3)_2 \rightarrow CpLi(NH_3)_3$ leads to longer (1.74, 1,8, 1.92, 2.16 Å) and hence weaker metal–ring bonds [76].

Traditionally, molecular structures are typically treated in terms of hybridization and electronic ligand effects. Both concepts, however, are of limited relevance to $CpML_n$ complexes. As a matter of fact, experimental L–M–L angles are often about 90° and are hence at variance with the classical predictions of 120° ($n = 2$) or 109° ($n = 3$). For example, the N–M–N angle of ca. 85° is characteristic of many tmeda–lithium compounds [72,79]. According to SCF calculations, the N–Li–N angles in $CpLi(NH_3)_2$ and $CpLi(NH_3)_3$ should be 95 and 97°, respectively [76]. Similarly, neither the four legged structure nor the electron construction of CpLi(12-crown-4) can be rationalized in classical terms [75]. Concerning the Cp–M bond hapticity changes in $CpML_n$, ab initio calculations on a series of the cyclopentadienyl aluminum compounds point to negligible (4–8 kJ mol^{-1}) energy differences between various hapticities (η^1, η^2, η^3, η^5) [18]. The underlying mechanism is definitely distinct from the fluxional mechanism suggested for beryllocene [80,81]. As another example, the pentahapto geometry of the Cp ring in the model compounds $CpAlX_2$ (X = H, OH, NH_2, OCF_3) or dimers $[CpAlNH]_2$ and $[CpAlO]_2$ cannot be explained via the electron-withdrawing nature of the X ligands thought to allow greater Al–Cp π-interactions. Ab initio calculations showed that, starting from an η^2 arrangement, 'both increasing and decreasing the degree of ionicity of the Cp–Al bond results in a shift to higher hapticity' [82]. In other words, the question about the force directing the hapticity change remains unresolved.

Finally, an intriguing case concerns the dimeric aluminum complexes $\{CpAlN(2,6\text{-}^iPr_2C_6H_3)\}_2$ [83], $\{(\eta^5\text{-}C_5Me_4Et)Al(Cl)_2\}_2$, and $\{(\eta^5\text{-}Cp^*Al(Cl)_2)\}_2$ [84] all of very similar coordination geometry about aluminium. It is noteworthy that the interplane distances (defined as the separation between the Cp plane and the N–N line in the former and the Cl–Cl–Cl plane in the latter) are 3.17 and 3.04 Å, respectively, much shorter than the corresponding sums of vdW radii (1.75 Å (Cp); 1.55 Å (N); 1.75 Å (Cl)) [38]. Thus, the observation of the η^5 structure signals that vdW attraction outweighs vdW repulsion. If the steric requirement is now enlarged by even just a small margin, e.g. by replacing one Cl with the methyl group (r_{vdW} 2.0 Å) [41] the structure changes to the η^3 mode in $\{\eta^3\text{-}Cp^*Al(Cl)(Me)\}_2$, due to the slippage of the Cp unit with the Cp–L_n interplane distance remaining nearly unchanged [85]. Upon replacement of another Cl in going to monomeric Cp^*AlR_2 (R = Me, Et, ^{i}Bu) [86], the hapticity is further decreased to η^2. The same scenario is found in the isolobal and isoelectronic complexes Cp^*MR_2, (M = Al, Ga, In) [77]. Actually it is not the chemical nature of the ligand that controls these changes, but instead the distance. In fact, the decrease in the interplane distance between geminal Cl–Cl–Cl and Cp in going from the Cp^*AlCl_3 fragment in $\{(\eta^5\text{-}Cp^*Al(Cl)_2)\}_2$ (with Al–$Cl_{bridged}$ and Al–$Cl_{tortial}$ distances of 2.34 and 2.15 Å, respectively) to the monomeric anionic species $[\eta^1\text{-}Cp^*AlCl_3]^-$ (Al–Cl distance 2.17 Å) [60], the Cp unit slips along the Cl–Cl–Cl plane giving η^1 coordination.

The interplane distance can also be affected by changing the acceptor strength of the central metal, noting similar changes in hapticity. Thus compare the η^5 mode in $[Cp^*AlCl_2]_2$ with the η^1 mode in $[Cp^*GaCl_2]_2$ [87] where the Cp-(geminal Cl–Cl–Cl)

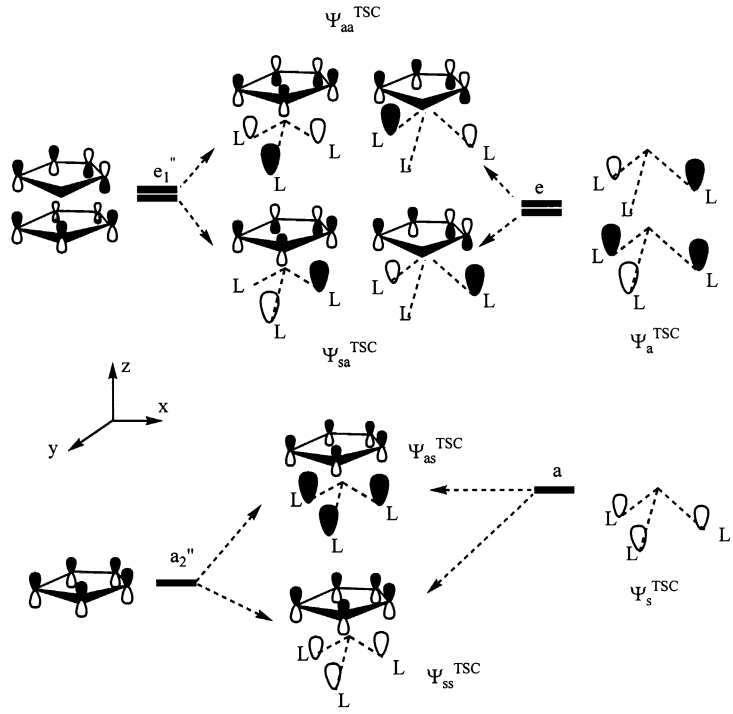

Fig. 4. Interaction scheme for the π Cp and the L_3 system TSC orbitals.

distance changed from 3.04 to 2.85 Å. Note also the large body of η^1-pentamethylcyclopentadienyl substituted boron compounds [88]. Finally, strong σ-donors entailing small M–L distances, can, because of strong vdW repulsion, reduce the Cp–metal interaction into ionic bonding as in the tris-alkyltin complex $[Cp]^-$ $[SnR_3]^+$ [89].

Fortunately, all these peculiar features are straightforwardly accommodated with the aid of the TSC concept. At first, the $\{L_n\}$ ligands in $Cp'ML_n$ form a united system of TSC orbitals from the Ls' lone p orbitals giving symmetric Ψ_s^{TSC} and anti-symmetric Ψ_a^{TSC}. These in turn are linearly combined with the symmetric (a_2'') and anti-symmetric (e_1'') orbitals of Cp yielding a second generation of TSC orbitals Ψ_{xy}^{TSC}, as depicted in Fig. 4 for the case of three σ ligands. As to the terminology, the first subscript refers to the symmetry of the combination of the orbitals, and the second one to the symmetry of the individual orbitals, where s and a mean symmetric and asymmetric, respectively. The individual orbitals have either more Cp′ or L_n character, depending on the energy levels of the participants. As a rule, the Cp′ π-orbitals are lower in energy than the TSC orbitals of the L_n system, for space reasons (cf. through-bond coupling in Cp and though-space coupling in L_n). Consequently, the bonding orbitals are more Cp based. Since all orbitals are filled, the bonding orbitals Ψ_{ss}^{TSC}, Ψ_{sa}^{TSC} determine vdW attraction, while the anti-bonding orbitals Ψ_{as}^{TSC}, Ψ_{aa}^{TSC} are responsible for vdW repulsion between Cp′ and L_n group.

Next, in Fig. 5, we combine the TSC orbitals with the metal AOs. Clearly, there is good overlaping between Ψ_{ss}^{TSC} and Ψ_{as}^{TSC} and the metal s and p_z, whereas Ψ_{sa}^{TSC} can interact only with the metal p_x and p_y. The result is four bonding MOs A, B, C, and D in which to house eight electrons. In filling A and B, two electrons each are donated from Cp′ and the L_n group. In filling C and D, however, it is important to note that Cp′ does not contribute four electrons, but a lesser amount depending on the participation of Cp′ in Ψ_{sa}^{TSC}. In summary there is a contribution of $(6-\delta)$ and $(2+\delta)$ electrons, respectively, donated from the Cp′ and L_n fragments, where δ is the contribution of electron density of L_n to Ψ_{as}^{TSC}. Thus, in the TSC picture, the eight-electron count is not altered in going from Cp′ML to Cp′ML_4, in contrast to the formal electron count increase from eight- to 14-electrons. Consequently, in the absence of d orbital participation, any counting rules in addition to the octet rule unnecessarily complicate the issue. The decrease in electron density from six- to $(6-\delta)$ electrons donated from Cp′ in going from Cp′M to Cp′ML_n is revealed in Cp–M distance lengthening. The case of the $CpLi(NH_3)_n$ complexes has been cited above. As another example, the M–Cp(centroid) distance of 1.74 Å in LiCp [90] is increased to 2.06 Å in the CpLi(12-crown-4) complex [75].

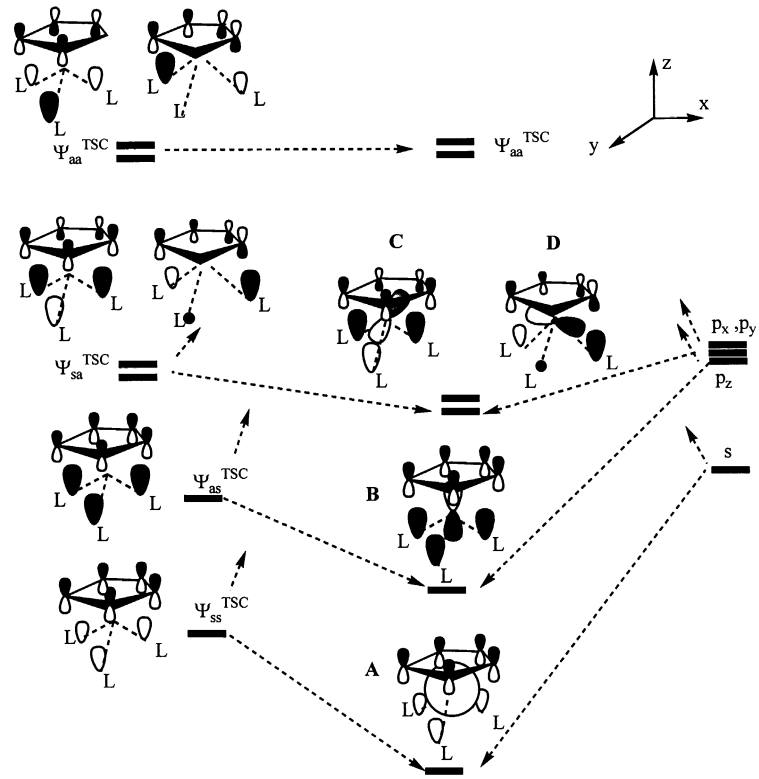

Fig. 5. Interaction scheme for TSC orbitals of the Cp-L_3 system and s,p metal AOs.

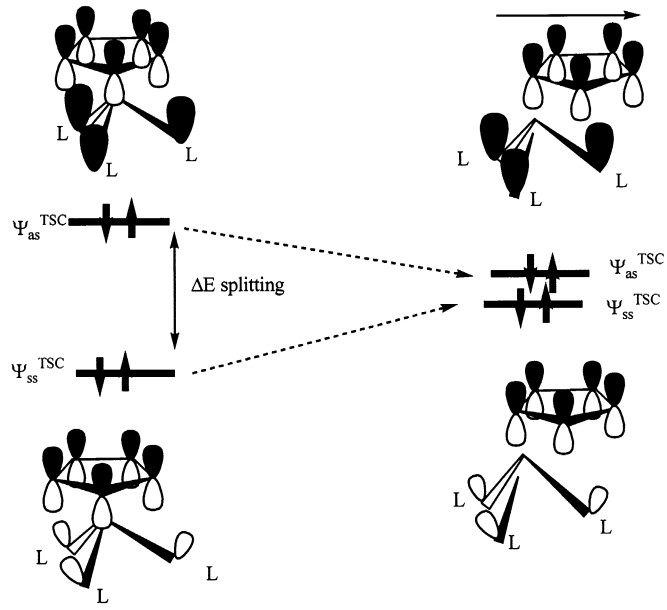

Fig. 6. Reduction of $\Psi_{as}^{TSC}/\Psi_{ss}^{TSC}$ splitting upon Cp slipping along the L–L–L plane (without metal contribution).

All these interactions of bonding orbitals not only stabilize the Cp′ML_n complex, but also lay the basis for interligand vdW attractions. Note that the linear $\langle \Psi_{ss}^{TSC} \mid s \rangle$ and $\langle \Psi_{as}^{TSC} \mid p_z \rangle$ interactions are the reason why the η^5-Cp′M geometry is preferred. This arrangement may be termed 'centrosymmetric', also if the L_n ligands do not lie on the M–Cp′(centroid) axis. The anti-bonding orbitals (Ψ_{aa}^{TSC}), for symmetry reasons, cannot interact with the (main group) metal AOs. In the case of Cp′ML_3, the electron density on these orbitals equals four electrons with the main portion $(4-\delta)$ electrons contributed from the L_n lone pairs and δ electrons from the Cp unit. This interaction, due to anti-bonding, results in a destabilization of $CpML_n$ and furthermore give rise to vdW repulsion between the Cp′ and L_n groups, depending on the ratio $(4-\delta)/\delta$. The stronger the interaction of the TSC orbitals between the Cp′ ring and the ligands behind the metal center, the higher lies Ψ_{aa}^{TSC}. The associated increase in the vdW repulsion provokes slippage of the Cp′ ring along the L_n plane. In this way the TSC orbitals interaction is weakened but the coplanar construction of the Cp′ π-orbitals and the Ψ_s^{TSC} orbital of $\{L_n\}$ is maintained. This is displayed in Fig. 6. Reverting to the example of [η^5-Cp*Al$(Cl)_3$]$^-$ above, EHMO simulations show that a reduction of the Al–Cl distance from 2.34 to 2.17 Å leads to a ca. 0.36 eV increase in the repulsive energy between Cp* and 3Cl. This amount is reduced to about 0.15 eV upon slippage of the Cp plane along the {Cl–Cl–Cl} plane.

Finally, depending on the value of δe (i.e. the extent of Cp π-orbital participation), the Ψ_{aa}^{TSC} orbital is the origin of the π-donor property of Cp′ML_n complexes,

particularly if L_n is a crown or cryptand ligand. Nucleophilic addition of other sandwich or half-sandwich complexes yields multidecker anions with encapsulated alkali metal counterions [91].

2.2. Metallocenes

2.2.1. Planar systems

The uniqueness of unsaturated Cp′M is rooted in the simultaneous availability of low-lying σ/π acceptor orbitals (Fig. 3) and (ligand-based) π-donor orbitals ($1e_1$ in Fig. 2). Therefore, with π donors such as Cp^- the anionic $[Cp_2Li]^-$ complex is attainable, and with σ/π acceptors such as Li^+ the cationic inverse sandwich complex $[LiCpLi]^+$ [23]. The orbitals' orientation is such that intercomplex bond formation is effective. For instance, the formation of the dimer $[CpLi]_2$ is highly exothermic ($\Delta E = -55$ kJ mol^{-1}) [92]. Ultimately, neutral polymeric $\{Cp'M\}_\infty$ structures of linear 'super-sandwich' or bent 'zig–zag' chains [23] are formed via centrosymmetric (η^5-Cp)-M-(η^5-Cp) links [16,77,90,93–95] reflecting the importance of the axial interaction between the π_{sym} Cp orbital and the metal s, p_z AOs (Fig. 7).

Attachment of another aromatic system, acting as a donor, to Cp′M yields the s^0p^0 sandwich complexes, in particular the metallocenes. Thus, adding anionic Cp^- or neutral benzene to LiCp to give $[LiCp_2]^-$ and BzLiCp is highly exothermic (-172 and -58.8 kJ mol^{-1}), according to ab initio calculations [92]. In these reactions, the π_{sym} (a_2'') orbital of the second Cp interacts strongly with the non-bonded $2a_1$ (or classical non-occupied sp) orbital of the CpM unit. The other two filled π-orbitals of the Cp′-system (e_1'' or π_{asym}) overlap with two anti-bonding ($2e_1$) orbitals of CpM, which are metal-like (largely metal p_x and p_y), thereby destabilizing the $\langle p_x \mid e_1'' \rangle$ and $\langle p_y \mid e_1'' \rangle$ interactions. Summed up, there are interac-

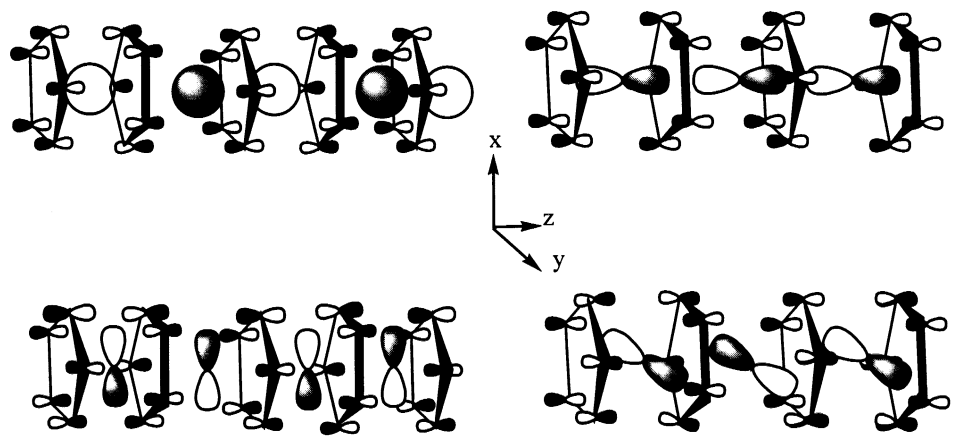

Fig. 7. The interactions of the π_{sym} Cp orbitals with the metal s or p_z AOs (top) and the π_{asym} Cp orbitals with the metal p_x or p_y AOs (bottom).

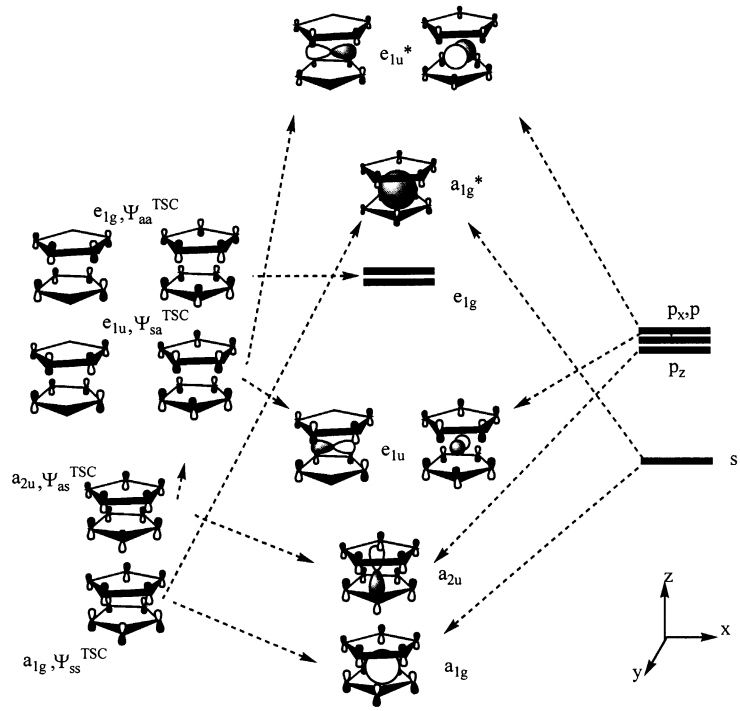

Fig. 8. Interaction scheme of two π Cp systems and the metal s,p AOs.

tions between (i) two metal sp hybrid orbitals and the π_{sym} orbitals of the two Cps′, and (ii) two orthogonal metal p orbitals with only one pair of the π_{asym} orbitals of each Cp′. In this description, however, it is difficult to accommodate the commonly found ring-slipped and bent structures.

In the TSC framework, the metal AOs interact with the π TSC orbitals combined from both Cp ligands, analogously to the Cp–L_n system above. The result is presented in Fig. 8. The TSC orbitals of the Cp–Cp system are Ψ_{ss}^{TSC} (a_{1g}) from $\{a_2'(1) + a_2'(2)\}$, Ψ_{sa}^{TSC} (e_{1u}) from $\{e_1'(1) + e_1'(2)\}$, Ψ_{as}^{TSC} (a_{2u}) from $\{a_2'(1) - a_2'(2)\}$, and Ψ_{aa}^{TSC} (e_{1g}) from $\{e_1'(1) - e_1'(2)\}$. The first two are the bonding orbitals relevant to vdW attraction, while the second two are the anti-bonding orbitals responsible for vdW repulsion between the Cp′ units. It may be emphasized that π TSC between the Cp rings is more effective than the corresponding interactions in the half-sandwich complexes. The Jahn-Teller splitting may be used as a criterion in this respect, which is as high as 1 eV for Cp_2Be (gas phase) and thus one order of magnitude higher than that found for half-sandwich CpBeL [71]. As another example, in Cp_2Mg, with an interplane distance of 4.0 Å, the difference between the e_{1u} and e_{1g} levels is 0.9 eV [96]. A simple EHMO analysis of the through-space interaction between the orbitals of two parallel Cp rings shows that the energy difference between the bonding and anti-bonding TSC orbitals is on the order of 0.25 eV and levels out, if the Cp-Cp interplane distance is increased from 4.0 to 4.5 Å (Fig. 9).

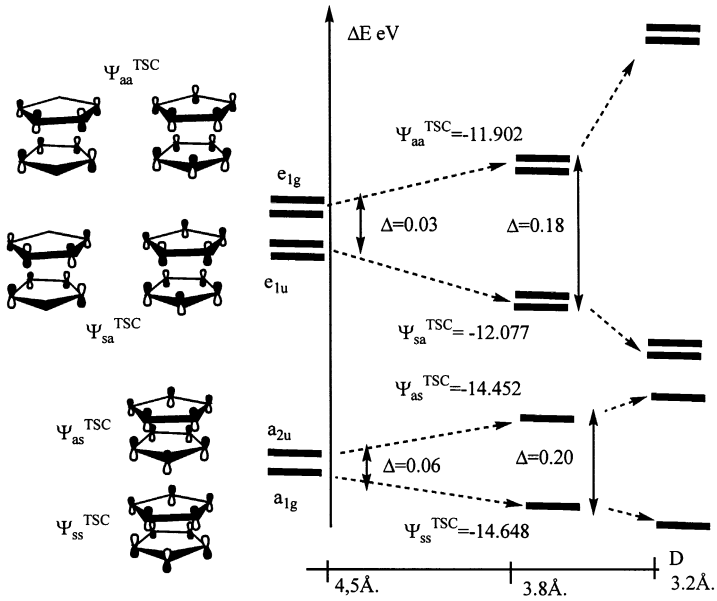

Fig. 9. Change in TSC orbital splitting (EHMO level) of two Cp systems upon decreasing the interplane distance *D*.

The interactions of Ψ_{ss}^{TSC}, Ψ_{sa}^{TSC} and Ψ_{as}^{TSC} with the metal s,p set form the bonding a_{1g}, a_{2u} and e_{1u} orbitals and the high-lying anti-bonding orbitals (Fig. 8). It should be emphasized here that the anti-bonding orbital (a_{1g}^{*}) formed by appropriate overlap of the symmetric combination (a_{1g}) of the two Cp rings is above the two degenerate e_{1g} orbitals in line with the diamagnetism of $[Cp_2Li]^-$ or $[Cp_2Na]^-$ etc. Otherwise these complexes would be paramagnetic.

As in the half-sandwich case, the axial (centrosymmetric) interactions $\langle \Psi_{ss}^{TSC} \mid s \rangle$ and $\langle \Psi_{sa}^{TSC} \mid p_z \rangle$between the metal and Cp are responsible for the η^5 bonding. In fact, the anions $[Cp_2Li]^-$ and $[Cp_2Na]^-$ exhibit highly symmetric sandwich structures with approximate D_{5d} symmetry [90,97,98]. If, however, the symmetry of the π_{sym} orbitals is changed by switching from $[(Cp)_2Li]^-$ to the boron-replaced analog $[(C_5BH_5)_2Li]^-$ [99] the ring-Li construction becomes asymmetric, despite the unchanged metal–ring distance. This result reflects the importance of the $\langle p_z \mid \Psi_{as}^{TSC} \rangle$ overlap to the Cp–M hapticity.

As an important outcome, there are eight electrons involved in the bonding in Cp_2M where each Cp ligand donates four electrons from π_{sym} and from one of the two π_{asym} MOs. The other four electrons are located on the two degenerate Ψ_{aa}^{TSC} orbitals and cannot participate in metal–Cp bonding. Their anti-bonding nature actually destabilizes the metallocene construction and, on the other hand, effects the π-donor property of $Cp_2'M$ giving rise to inter-complex interactions.

M–Cp bond weakening due to the reduction of the electron density from six to four electrons enhances the Cp–M distance in $[Cp_2M]^-$ relative to CpM (from 1.81

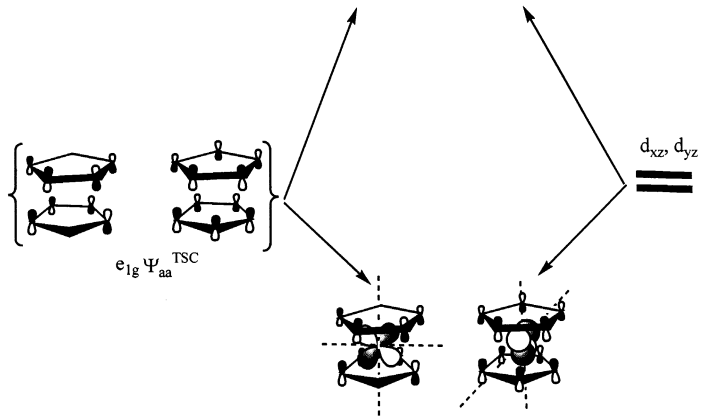

Fig. 10. The interaction of the e_{1g} orbitals of a two Cp system with d_{xz}, d_{yz} of a d metal.

to 2.10 Å for Li, and from 2.25 to 2.43 Å for Na) [90]. A similar increase from 1.44 to 1.5 Å is seen in going from CpBeCl to Cp_2Be [25,66], with C_{5v} symmetry maintained. The weak M–Cp bonding entails a small rotational barrier of 130 J mol^{-1} of the Cp fragment, which is one order of magnitude smaller than that for ferrocene [100]. In the latter, there is good overlap between Ψ_{aa}^{TSC} and d AO of iron. The small rotational barrier in turn favors flexible ring orientations. Thus, the co-planar structure of Cp_2Mg with staggered rings (D_{5d}) in the crystalline environment [101] is marginally more stable by about 125–200 J mol^{-1} than the eclipsed conformation (D_{5h}) found in the gas phase [96].

The stronger the TSC orbital splitting, the more anti-bonding are the Ψ_{as}^{TSC} orbitals. Removal, therefore, of electron density from the latter highly increases the attraction between the two Cp groups. However, the simultaneous raise of the other filled anti-bonding Ψ_{aa}^{TSC} orbitals, provokes (uncompensatable) vdW repulsions. On the other hand, the loss of TSC upon increasing the Cp′ interplane distance, lowers both the Ψ_{as}^{TSC} energy and the attractive interaction between two Cp groups. The delicate interplay of these effects is the foundation of the structural diversity of the metallocenes.

2.2.2. Distortions

For the transition metals, as is well known, the d electron configuration controls the geometry of their metallocenes. These have ordinarily parallel ring structures with interplane distances considerably below 4 Å [102], which in the case of ferrocene just equals that of graphite (3.36 versus 3.35 Å). In terms of Fig. 10, such small distances bear witness to the important role played by the $\langle \Psi_{aa}^{TSC} \,|\, d_{\pi} \rangle$ interaction, donating from high-lying Ψ_{aa}^{TSC} into metal AO. Thereupon, electron–electron repulsion is minimized by partially converting the initial vdW repulsion into vdW attraction.

In the absence of d orbitals, the Cp–M bonds are weaker enabling the occurrence of bending [31] or slipping ultimately making the symmetric parallel ring structure rather the exception than the rule. In the series of the alkaline earth metallocenes, magnesocene is in fact the only one with parallel ligand planes (D_{5h}) [103]. But there the strive for bending and/or slipping of the Cp rings is also obvious from the vibrational frequencies of the symmetric and anti-symmetric ring tilts [100]. Since in Cp_2Mg the metal–ring distance is 2.0 Å, one may conclude that the distortions typical of the alkali and alkaline earth metallocenes occur with increasing deviations from that mark. The tendency towards distortions is rooted in the filled Ψ_{aa}^{TSC} orbitals enabling vdW repulsion between two Cp planes and, since being the HOMOs, create favorable conditions for the Jahn–Teller effect. This latter effect may have great impact on both the stability and reactivity of Cp_2M complexes.

2.2.2.1. Slippage. A case study of a slip-sandwich structure is beryllocene [104,105]. This compound prefers a η^1-η^5-coordinated conformation of C_s symmetry with parallel ring planes separated by 3.375 Å [106]. Interestingly, this distance is very close to the interplane distance in graphite (3.35 Å). Clearly, such a small interplane distance, significantly below twice the vdW radius for aromatic carbon, does not allow face-to-face approach of the Cp rings. The reason is the high-lying filled anti-bonding Ψ_{aa}^{TSC} orbitals giving rise to strong Cp–Cp vdW repulsion (Fig. 9). On the other hand, expanding the inter-ring distance would break off the Cp–Be interactions because of the small size of beryllium. According to calculations, a slight expansion to 3.7 Å corresponds to 105 kJ mol^{-1} loss in energy [68].

The situation is remedied by moving one of the rings sideways. In this way (i) TSC splitting (e_{1u}/e_{1u}^*), and hence vdW repulsion, is reduced, and (ii) there is a compensation since p_x changes its partner from e_{1u} to e_{1g}, upon inversion of one e_{1g} and one e_{1u} (Fig. 11). The other orbitals involving s, p_z and p_y remain unaltered. In this way the destabilizing effect of the Ψ_{aa}^{TSC} orbitals is lifted. It has been calculated that the transformation of (η^5-Cp)$_2$Be (D_{5d}) into (η^1-Cp)(η^5-Cp)Be (C_s) gains 42.7 kJ mol^{-1} [68]. Another consequence of the above compensation is the dynamics of the $\eta^5 \rightarrow \eta^1$ changes with activation barriers as low as 4–12 kJ mol^{-1} [81,107]. Similar slipped structures have been found such as the η^1–η^6 structure of [$C_6H_5BeC_6H_6^+$] [21] and the η^1–η^5 structure of [(^{i}Pr)$_4C_5H]_2Zn$], with a Zn–ring(centroid) distance of 1.92 Å [108]. If the metal radius is further decreased as in Cp_2B^+ (Cp–B distance $\approx$1.35 Å), the slipped-sandwich transforms into [(η^5-Cp*)(σ-Cp*)B^+] [109].

2.2.2.2. Bending. In the absence of bulky substituents, parallel Cp planes in η^5-arrangements are found for (s^0p^0) metallocenes for interplane distances about 3.7–4.0 Å, as noted above. This is the case, e.g. for cationic $[Cp_2Al]^+$ (3.68 Å) [60,110] anionic $[Cp'_2Li]^-$ (ca 4.0 Å) [89], or neutral $[Cp_2Mg]$ (4.0 Å) [96]. Slight bending occurs in (η^5-tris(trimethylsilyl)cyclopentadienyl)$_2$Mg with an average Cp–Mg–Cp angle of 171,1° and the Mg–Cp(centroid) distance 2.02–2.04 Å [111]. The striving for parallel Cp planes appears to control the Cp arrangements around the metal in linear or non-linear ('zig–zag') polymeric structures (Fig. 12). The

preference of the planar construction of two Cp rings around Na^+ is confirmed by the easy transformation of the monomeric silicon-bridged anionic sodocene complex $[(allyl)_2Si(C_5H_4)_2Na]^-$ into polymeric chains in which Na cations bridge

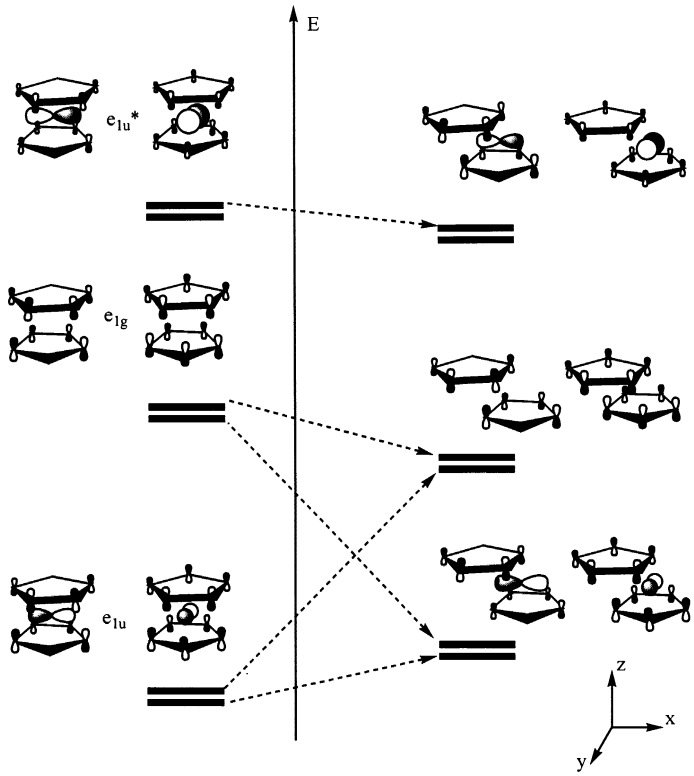

Fig. 11. Correlation diagram for Cp slipping in Cp_2M.

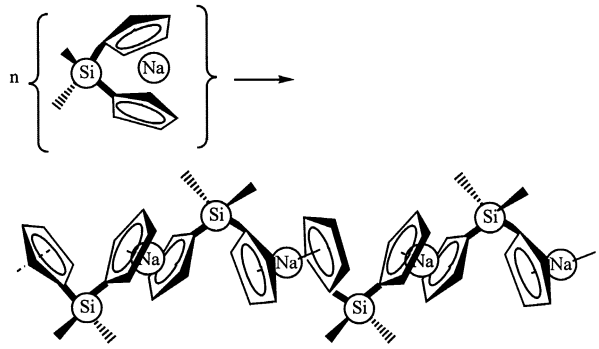

Fig. 12. Striving for parallel ring orientations about sodium in the polymerization of $[(allyl)_2Si(C_5H_4)_2Na]^-$ units.

$[(allyl)_2Si(C_5H_4)_2]^{-2}$ units [62]. The interplane Cp–Cp distance of 4.7 Å involved is identical to that in sodocene. Although the ionic radii of Na and Ca are very similar, it is interesting to note that Cp_2Ca forms only bent structures both in the gas phase or as a polymer in which Ca is surrounded by four Cp groups ($\eta^5,\eta^5,\eta^3,\eta^1$) [112]. Also, the Cp–M distances are similar for both metals. This unexpected behavior may be traced to the three-times larger polarizability of Ca^{2+} compared to Na^+ [113] in line with the higher s orbital radii of the former (2.16 vs. 1.71 Å) [114]. Note finally that all other (s^0p^0) metallocenes with interplane distances exceeding, say, 4.7 Å are bent.

Classically, attempts to explain the bending in the Cp_2M (s^0p^0) systems invoke hybridization and electronic ligand effects. If, however, Cp_2Ca is bent due to 'empty low-lying d orbitals that can be used for bonding' [115], why in polymeric $\{CpLi\}_\infty$, is Li not bound exactly on the line between the centers of two adjacent Cp rings [23]? Further, relativistic effects [100] should be of minor importance for light atoms. An alternative explanation utilizes non-bonded interactions, especially attraction between the Cp ligands [26]. In these terms, the bending potential is determined by cation-polarization effects, which increases with the metal cation size [116,117]. Since the interaction of the Cp rings with a polarizable metal center is equivalent to the interaction with vacant orbitals, the reason for bending ought ultimately to be rooted in intramolecular electronic forces [33]. Recently, bent structures could be reproduced by applying a molecular mechanics force field model on the assumption that only non-bonded interactions are operative and electronic factors play no role [34]. It transpires, however, that the global minima of bent structures can only be recognized with higher theory, in view of the very small energy differences between coplanar and bent structures [115].

In summary, the main reason for bending should be sought in vdW attractive forces between the Cp rings, in the absence of the interaction between the metal orbitals and the degenerate anti-bonding occupied Ψ_{aa}^{TSC} orbitals. At least two questions are yet to be answered. How can the mechanism of bending be envisaged? What are the nature of the attractive or non-bonded interaction forces and the cation-polarization effect?

Simple EHMO level calculations on Cp'_2M systems show that the through-space interaction for parallel Cp′ planes' configuration levels out for Cp interplane distance higher than 4.7–4.8 Å (Fig. 9). The loss in stability from TSC between the Cp π-systems can be partly counteracted by Cp slippage around the metal center. In this way the borders of the π-systems move together resulting in a renewed $\Psi_{aa}^{TSC}/\Psi_{sa}^{TSC}$ energy splitting (ca 0.15–0.1 eV) until the Cp planes' border distance (λ) reaches a limit of about 4.0–4.3 Å, independent of the Cp(center)–metal distance (Fig. 13). Of course, this distance λ cannot be smaller than 4.0 Å due to vdW repulsion between the Me groups, in agreement with experiment. This value is not reached in the case of bulky substituents exercising larger vdW repulsions.

Since the vdW repulsion limits the extent of bending, a relationship can be suggested between the Cp′ borders' distance λ, the Cp(plane)–metal distance L, the π-orbital ring radius R_{Cp} of Cp′ and the tilt angle α (Fig. 14):

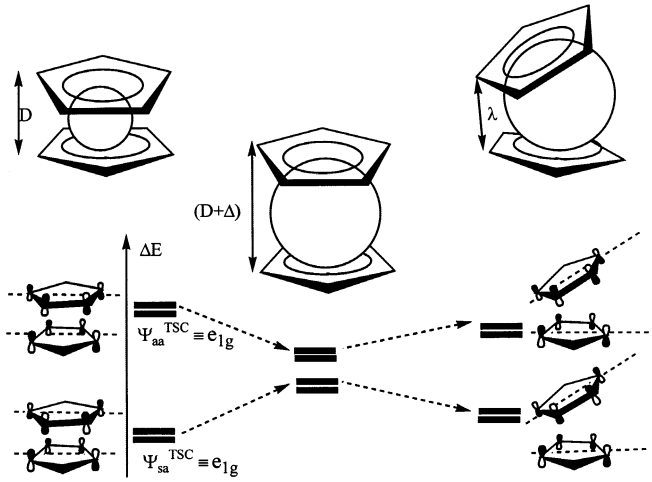

Fig. 13. Effect of bending of the Cp planes by extending the interplanar distance from D to $(D + \Delta)$ on the splitting of e_{1u} and e_{1g} orbitals.

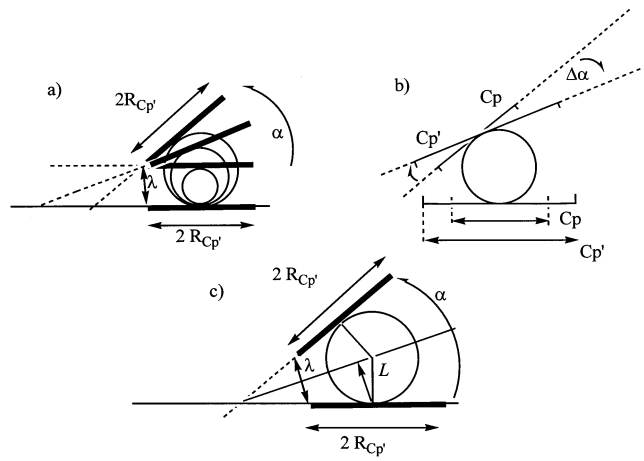

Fig. 14. Degree of bending varying with size of (a) metal and (b) Cp′ ligand. (c) geometric parameters: α = angle between the ring planes; λ = border–border distance; L = metal–ring(centroid) distance; $R_{Cp'}$ = radius of Cp′ ligand.

$$L\cos(\alpha/2) = \lambda/2 + R_{Cp'}\sin(\alpha/2)$$

Or, since $\alpha/2$ is relatively small, this approximates to a linear relationship,

$$L = \lambda/2 + R_{Cp'}\,\alpha/2 \text{ or } \alpha = -\lambda/R_{Cp'} + 2L/R_{Cp'}$$

This equation implies a linear dependence between α and L as found by Timofeeva et al. [26] who, however, used the (related) M–C(Cp) distance parameter. (The difference between the distances M–C(Cp) and M–Cp(centroid) plane is about 0.27

Å [54]). Furthermore, if L involves a constant Cp radius, a linear trend between the tilt angle and the metal ionic radius is expected and observed [33,103]. Such relationships based on the crystallographic ionic radii should not be taken too seriously, however, in view of the ambiguity of this parameter (e.g. its coordination number dependence).

The effect of bending on the orbital geometries and energies is sketched in Fig. 15, assuming bending about the y-axis. Thus, the interactions of the s and p_y metal orbitals are unaffected, i.e. the orbitals A, C, and E remain unchanged. Also only slightly changed is the interaction of the p_z orbital (B), also implying that in the bent metallocenes the η^5-bonding mode wants to be maintained. However, the metal tends to be pushed out of the 'den' defined by the displacement of the ring

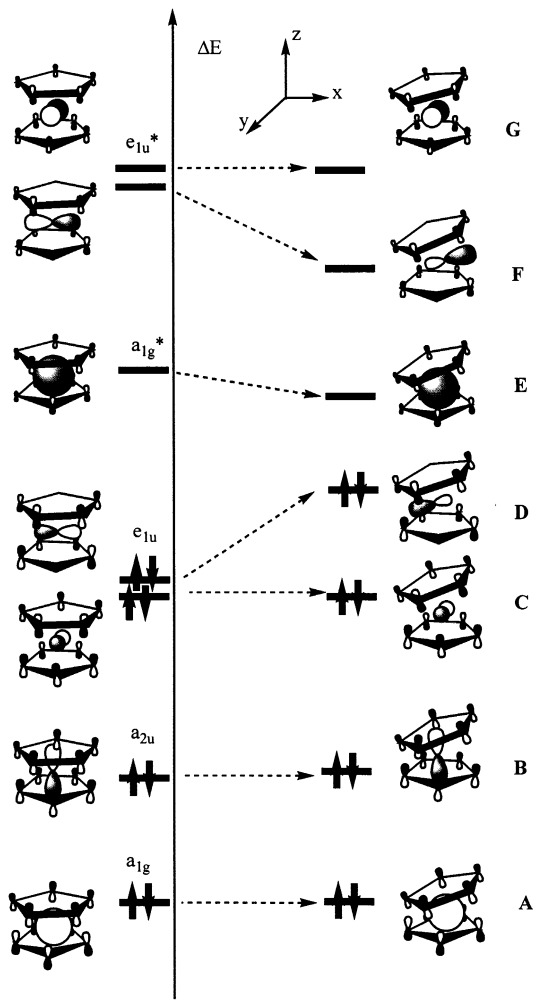

Fig. 15. Change in orbital geometries with bending.

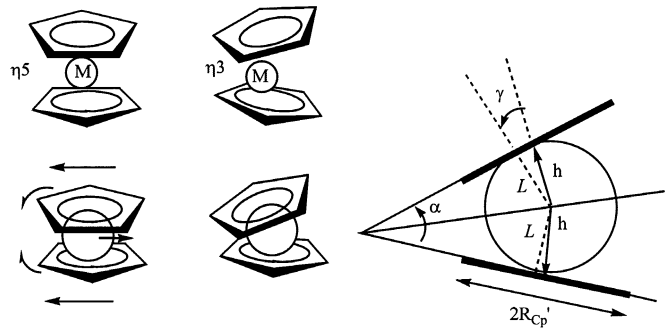

Fig. 16. Change in hapticity upon bending with the metal slightly pushed out: h = distance between metal and Cp center; γ = tilt angle; for the other symbols see Fig. 14.

centroid from the normal to the ring plane or the tilt angle γ (Fig. 16). For example, the Cp* rings in the bent complexes Cp^*_2Ca, Cp^*_2Sr and Cp^*_2Ba are ca. η^5 bonded [33], but γ increases in going from Ca to Ba in the range 0–3° [115]. Such a displacement of the metal atom may be understood in terms of the strive for the planar conformation of the Cp planes to achieve the highest possible TSC.

The largest changes concern the orbitals D (e_{1u}) and F (e^*_{1u}) including the metal p_x. The former is bonding and contributes to the stability of the complex, while the latter is anti-bonding, empty and more metal-like (towards sp^2). It is this orbital F that can act as an acceptor and engage in the mechanism of polarization. There are interrelations between the distance between the Cp planes, the size of the cation, the angle between Cp planes, and the metal polarizability. In this context, the relationship between the cube root of polarizability and the atomic size should be noted [118].

Clearly, of primary importance here is the orbital F. It can accept a 'lone pair' from other molecules, imitating the sp^2 character of this orbital. With mono- or bidentante Lewis bases, therefore, the s^0p^0 metallocenes can form monomeric or polymeric adducts [33,112]. Even Cp_2Mg, which is planar in the ground state, but with little energetic difference between planar and bent conformations, forms the reversible adducts Cp_2MgL where L = tmeda, thf, diox, PMe_3, etc. [100]. Somewhat more stable are adducts with other Group 2 metals such as tetrahedral $Cp'_2M(base)_2$ (M = Ca, Ba, Cp′ = ^{t}BuCp) [119], trigonal [η^2-$Cp_2Cd(tmeda)$], η^1-$Cp_2Cd(PMDETA)$ (PMDETA = $(Me_2NCH_2CH_2)_2NMe$) [120], or the mono adducts $Cp_2M(OEt_2)$ [121], [Cp^*_2Ca-PEt_3] [122], $Cp'_2M(thf)$ {Cp′ = C_5H_3-1,3-$(SiMe_3)_2$, M = Ca, Sr} [78], [$Cp^*_2Ca(OEt_2)$], and [$Cp^*_2Ca(CO)$] [121]. Bent metallocenes can also bind soft bases giving, for instance, [$Cp^*_2Ca(MeC{\equiv}CMe)$] [121] and metallocene–olefin complexes. Ab initio calculations reveal weak interactions between $[Cp_2Na]^-$ and ethylene, with a bonding energy of 10.9 kJ mol^{-1}. However, a very shallow minimum has been found only for a C_2-symmetric species. The ethylene molecule is twisted in order to avoid repulsions with the Cp rings and shows long $C\cdots Na^+$

contacts of 3.79 Å, which are longer than the sum of the vdW radii. It is presumed that such weak interactions play an important role in addition reactions of organosodium compounds to alkenes and in ion-pair polymerization mechanisms [62].

Bent (s^0p^0) metallocenes have an ambiguous character. On the one hand, they have two (distorted because of bending) 'lone pairs' on Ψ_{aa}^{TSC}, which are the HOMOs responsible for base properties. On the other hand, they are acceptors via the F orbital. The combination of these properties gives rise to the formation of polymeric structures. Thus, in solid Cp_2Ca, each Ca ion is surrounded by four (bonded η^5, η^5, η^3, η^1) Cp rings [112]. Similar 'agostic' intermolecular interactions are found in Cp_2^*Ca and Cp_2^*Ba polymers. In the latter, the coordination sphere about Ba consists of two η^5-Cp rings and one η^1-Cp ring [33,123].

It seems strange at first sight that a bent (s^0p^0) metallocene should accept ligand electron density since it is electronically saturated if each Cp anion donates four electrons (see above). This issue is reconciled by the TSC concept by analogy to the $CpML_n$ systems. For nucleophilic attack at a bent sandwich complex, the σ orbital (either the lone pair of a single ligand or the Ψ_s^{TSC} orbital of two donor ligands) interacts with the acceptor orbital F (Fig. 17(a,b)). In this way the combined system $\{2Cp + L_n\}$ forms a second generation of TSC orbitals, Ψ_{sas}^{TSC} and Ψ_{saa}^{TSC} (Fig. 17(c)) as symmetric and anti-symmetric combinations of one of the degenerate Ψ_{sa}^{TSC} orbitals (Fig. 13) of the two bent Cp units and the σ orbital (in general Ψ_s^{TSC}) of the L_n group. Subsequent overlap of Ψ_{sas}^{TSC} and metal p_x orbitals, creates a new bonding orbital (Fig. 17(d)), which houses electron density equal to two electrons. Of this, only $(2-\delta)$ electrons derive from the two Cp π systems and δ electrons from the donor ligand(s). Conversely, only δ electron density from two Cp π systems contributes to the corresponding filled anti-bonding Ψ_{sas}^{TSC}, which has, therefore, more donor ligand character. Along these lines the octet rule is preserved. Note that the smaller donation from Cp weakens the Cp–metal bonding reflected by a lengthening of the Cp–metal distance as well as an increased bending angle (α) between the two Cp planes.

Because of the notable energy differences between Ψ_{sa}^{TSC} of two Cps′ and Ψ_s^{TSC} of L_n, the ratio $\delta/(2-\delta)$ is small, and the total electron density donated from the Cp units is almost eight electrons. Consequently, the Cp–metal bond is not destabilized greatly. In fact, adduct formation does not change the metal–carbon distances very much at all. As an example, upon coordination of thf to Cp'_2M $\{Cp' = C_5H_3\text{-}1,3\text{-}(SiMe_3)_2$, $M = Ca, Sr\}$ to give $Cp'_2M(thf)$, the metal–carbon distance is decreased from 2.68 to 2.61 Å for Ca, and from 2.8 to 2.75 Å for Sr. The corresponding changes of the interplane angle α are from 26 to 40.9° for Ca and from 31 to 46° for Sr [78]. Finally note that the distance between the borders of the Cp rings limits the bending and the number of ligands that can be added. Thus, the degree of maximum thf solvation observed in the metallocenes $Cp_2^*Ca(thf)_2 > Cp_2^{3i\mathrm{Pr}}Ca(thf) > Cp_2^{4i\mathrm{Pr}}Ca$ appears to be related to the order of the steric bulk of the rings $Cp^* < Cp^{3i\mathrm{Pr}} < Cp^{4i\mathrm{Pr}}$ [124].

2.3. Tris(Cp) complexes

We have seen that bending of (s^0p^0) metallocenes creates σ acceptor properties (from anti-bonding F). In addition, if bending is appreciable, the anti-bonding orbital G (Fig. 15) can also be utilized, making the complex a π acceptor. In this case not only (one or two) σ donor ligands can attack, but also ligands such as Cp anions, affording tris-Cp'_3M compounds. This tendency is obvious in the polymeric metallocenes, such as $\{Cp_3Ba\}^-_\infty$ [125], $\{Cp^*_2Ba\}_\infty$ [123], $\{Cp_2Ca\}_\infty$ [112] and the layered crystal structure of the cesium triple-decker complex $[PPh_4][Cs_2Cp_3]$ [126]. In all these cases the interplane angle and the M–Cp distance are large enough to accommodate another Cp unit.

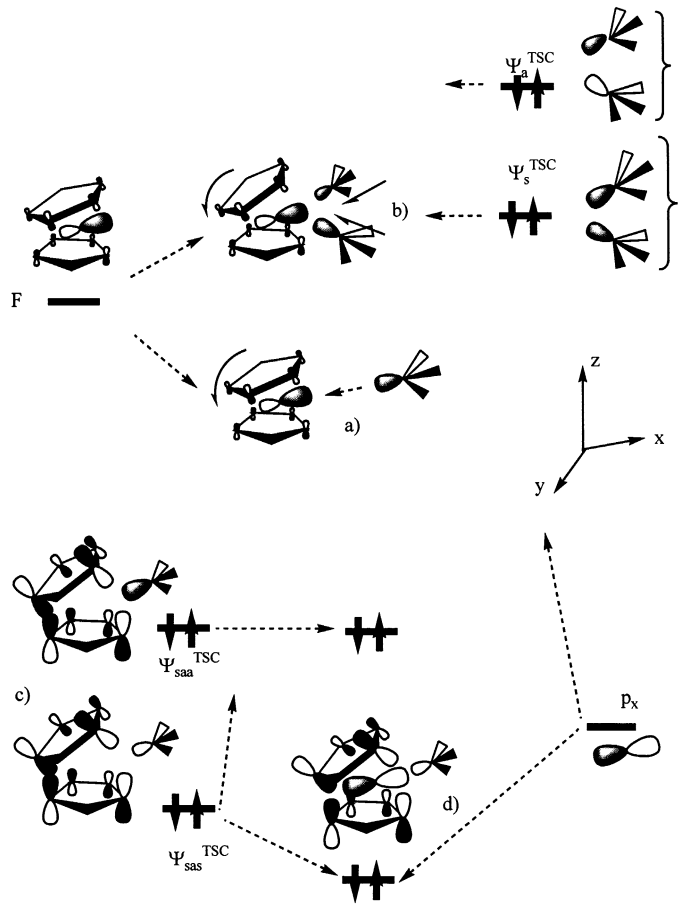

Fig. 17. Interaction of the metallocene orbital F (Fig. 15) with (a) one donor, and (b) two donors. (c) The adduct bonding orbital Ψ_{sas}^{TSC} formed from Ψ_{as}^{TSC} of two Cp′ units and the σ ligand orbital; (d) its interaction with metal p_x.

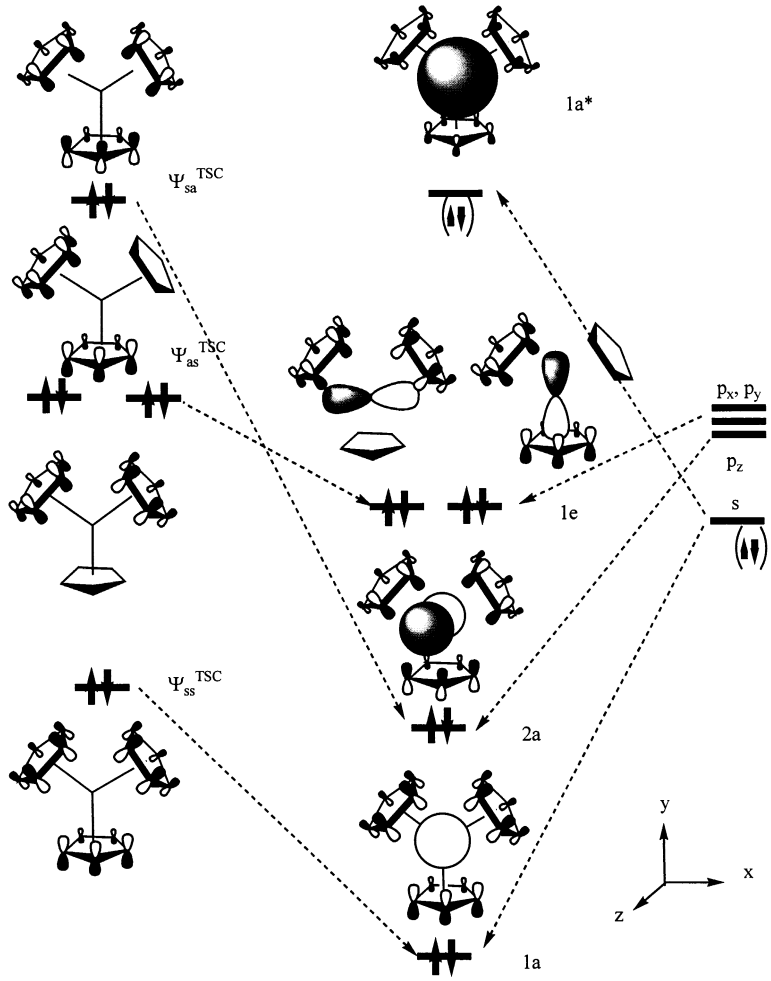

Fig. 18. The main interactions in a Cp_3M system.

Genuine tris compounds Cp'_3M can be obtained from Cp ring metathesis between Cp^*_2Ca and Cp_3Ln (Ln = La, Nd) complexes to give (η^5-$Cp^*_2\eta^5$-Cp)Ln [127]. The channel or 'paddle-wheel' structure [128] allows maximal through-space π interactions between the Cp ligands according to the main bonding interactions, depicted in Fig. 18, as follows: (i) three π_{sym} orbitals of each Cp unit form three TSC orbitals, viz. the bonding Ψ_{ss}^{TSC} and two anti-bonding Ψ_{as}^{TSC} orbitals (Fig. 18, left). The first one interacts with the metal s orbital, forming the low-lying bonding MO 1a. Its high-lying anti-bonding counterpart 1a* is the LUMO. (ii) The p_x and p_y orbitals, featuring a degenerate pair of D_{3h} symmetry [129], interact with the degenerate pair (Ψ_{as}^{TSC}) orbitals of the appropriate symmetry to give the bonding orbitals 1e. (iii) The three degenerate π_{asym} orbitals of Cp form six TSC orbitals, but

only one, namely Ψ_{sa}^{TSC}, can interact with the metal p_z orbital, around which the triangular arrangement is grouped. Not shown in Fig. 18 are five other filled TSC orbitals derived from different combinations of two π_{asym} orbitals of three Cp units. From symmetry, they cannot participate in metal–Cp bonding. Four of them, however, due to anti-bonding, are responsible for vdW repulsion between the Cp′ groups. All metal s,p orbitals are filled, with each Cp′ unit providing, formally, 8/3 electrons.

Both the hapticity and the Cp′(normal)–metal–Cp′(normal) angles are controlled by the distances between the borders of the rings through vdW attraction. We have analyzed the variation in TSC splitting of the Cp π orbitals upon decreasing the Cp(centroid)–dummy atom (i.e. the metal position) distance by simple EHMO calculations. At distances below 3.5 Å, TSC splitting becomes noticeable, reaching a value of about 0.4 eV at 2.5 Å. Below this, TSC splitting increases sharply to 2.3 eV at a distance of about 2.2 Å because of border–border repulsion. Decreasing the metal–Cp plane distance does not only increase vdW repulsion between the Cp borders but also increases the destabilizing effect of the filled anti-bonding TSC orbitals that do not participate in Cp–metal bonding. This effect is counteracted by lowering the hapticity through slippage of one, two or all three Cp′ groups in the direction perpendicular to the normal of the metal–Cp plane.

The paddle-wheel arrangement of η^5-bonded Cp groups is found in (η^5-$Cp^*_2\eta^5$-Cp)Nd [127], (η^5-Cp*)$_3$Sm, and (η^5-Cp*)$_3$U [130] with similar metal–Cp plane distances of 2.51–2.52 (Nd), 2.55 (Sm), and 2.58 Å (U). In these complexes, the border–border distance lies in the range 2.2–2.3 Å, which is the lower limiting value because of vdW repulsion. Therefore, upon taking either a larger ligand or a smaller metal ion, the geometry is changed through tangential slippage giving stepwise η^3 or even η^1 coordination. This is illustrated in the top of Fig. 19(a,b). Such modifications are observed, e.g. for sodium upon replacing Cp* by fluorenyl (Flu) forming the $[(\eta^1\text{-Flu})_3Na]^{2-}$ fragment with the metal–Cp plane distances maintained at ca. 2.5 Å [131]. (This is, however, not meant to say that Flu models a big substituted Cp ligand). Other examples are polymeric $\{(\eta^5\text{-Cp})_2(\eta^1\text{-Cp})Sc\}_n$ ($L = 2.19$ Å) [132] and a series of substituted Al–Cp compounds, $(Cp)_3Al$, $(MeC_5H_4)_3Al$, $(1,2,4\text{-}Me_3C_5H_2)_3Al$, $(1,2,3,4\text{-}Me_4C_5H)_3Al$ with the carbon on each ring closely bound to the aluminum at distances 2.016–2.161 Å. Ab initio calculations on model cyclopentadienyl–aluminum compounds point to negligible (4–8 kJ mol^{-1}) energy differences between different ring hapticities [18]. In $(1,2,4\text{-}Me_3C_5H_2)_3Al$ for instance one ring is η^5 coordinated and the other two are η^1. Pure η^1 coordination is found in (η^1-Cp*)$_3$Ga ($L = 2.037$ Å) [133] and in (η^1-Cp)$_3$Ga ($L = 2.05$ Å) [134,135].

If, conversely, the metal–Cp plane distance is larger than, say, 2.5 Å (Fig. 19(c)), the stabilization of the complex through TSC levels off. This is counteracted by the tendency for Cp rings to slip around the metal sphere, against each other. Thereupon both the Cp(centroid)–metal–Cp(centroid) angle and the Cp plane border distance are decreased, finally giving a pyramidal structure (d). This conformation is suitable to form polymeric links with a tetrahedral arrangement of Cp groups, as in $\{\eta^5\text{-}Cp_3Ba\}^-_\infty$ with an average Ba–Cp(centroid) distance of 2.9 Å [125] (Fig. 19, bottom).

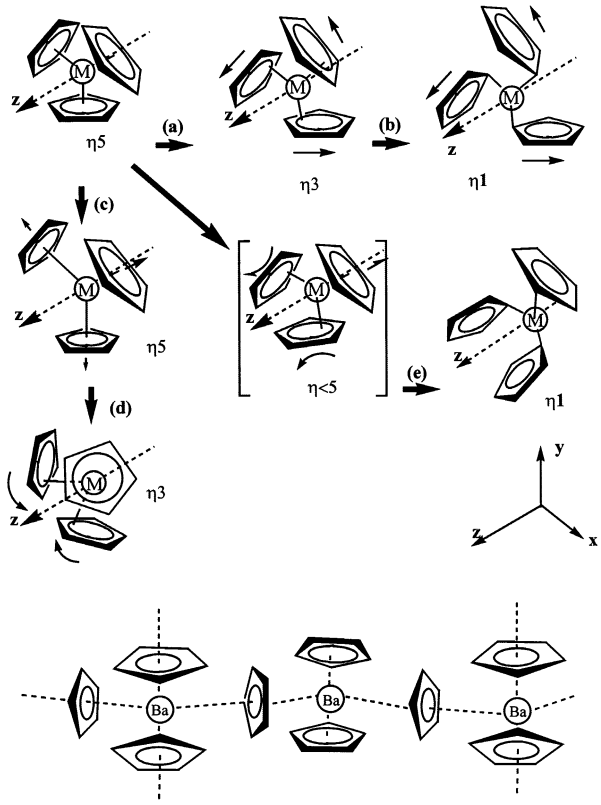

Fig. 19. Various structures derived from $(\eta^5\text{-Cp})_3M$. Decrease in L (or increase in $R_{Cp'}$) for s^0p^0 (path a,b forming the trigonal planar structure) and for s^2p^0 (path e forming the dipper structure); increase in L for both systems (path c,d). Bottom: $\{Cp_3Ba\}^-_\infty$ structure.

3. s^2p^0 metal systems

3.1. Half-sandwich complexes

The s^2p^0 Cp′M fragment is electronically saturated (eight electron rule), with filled $1a_1$, two $1e_1$, and $2a_1$ MOs (Figs. 1 and 2). The HOMO ($2a_1$), essentially non-bonding metal sp, is responsible for the σ donor property of the complex. The LUMO can be either two degenerate (e_2, or π* of Cp′) orbitals [61] or the anti-bonding ($2e_1$) MOs, which have more metal–like character (p_x, p_y). However, only $2e_1$ can display σ/π acceptor properties. The relative ordering of the $e_2/2e_1$ levels depends on the Cp′–metal distance.

The eight electron Cp′M complexes are well represented by the formula [Cp′M:], emphasizing the lone pair (on $2a_1$), which is perpendicular to and opposite to the Cp′ plane (Fig. 3). The position of the lone pair at the negative end of the molecule is revealed by significant experimental dipole moments, such as 2.2 D for Cp*In [136].

The species [Cp′M:] can exist without extra ligands as a nido-cluster of C_{5v} symmetry [137]. This structure is encountered with Group 13 and 14 metals in neutral $Cp^*Al^{(I)}$, $Cp^*Ga^{(I)}$, $Cp^*In^{(I)}$, $Cp^*Tl^{(I)}$ [138,139], Cp′Ga [140], (η^5-$P_3C_2^tBu_2$)In [141], or cationic $[Cp^*Ge]^+[BF_4]^-$ [10,142], $[Cp^*Sn]^+[BF_4]^-$ [10,143], and $[Cp^*Pb]^+$ $[BF_4]^-$ [144].

3.1.1. σ donor properties

The electronic construction of [CpM:] resembles a free carbene, occurring in both singlet and triplet states. The singlet–triplet state of Ga^+ may be represented by $Cp^*{\equiv}Ga^+{-}ML_n^- \leftrightarrow Cp^*{=}Ga{=}ML_n$ [145]. In the triplet exited state the complex can act as a bridging ligand similar to carbon monoxide as in $(CO)_3Co[\mu_2\text{-}(\eta^5\text{-}Cp^*Ga)]_2Co(CO)_3$ and $(CO)_3Fe[\mu_2\text{-}(\eta^5\text{-}Cp^*Ga)_2\mu_2\text{-}(\eta^3\text{-}Cp^*Ga)]$ $Fe(CO)_3$ [145]. In the singlet ground state, [CpM:] is typically a Lewis base [146] and can act as a terminal σ donor ligand in transition metal chemistry, again like carbon monoxide. To this category belong $Cp^*Ga(Fe(CO)_4)$, $Cp^*GaCr(CO)_5$ [145], $Ni(Cp^*Ga)_4$, *cis*-$M(Cp^*Ga)_2(CO)_4$ (M = Cr, Mo) [147], $Cp^*InCr(CO)_5$ [148], $Cp^*BFe(CO)_4$ [149,150], and $Cp^*AlFe(CO)_4$ [151]. For the complexes in solution, the η^5-bonding mode of the Cp′ ring and a linear Cp′(centroid)–M–L vector are common. In the solid state, some deviations from linearity are found, as in [$Cp^*InCr(CO)_5$] (157.7°) and [$Cp^*GaCr(CO)_5$] (167.5°). Repulsive intramolecular interactions between the Cp* methyl groups and the surrounding $CO_{equatorial}$ ligands have been invoked as the reason for these deviations [148]. This interpretation, however, is inconsistent with the order of the interplane (Cp*-4 $CO_{equatorial}$) distances which is 4.753 Å in the former and 4.315 Å in the latter. An even smaller distance of 4.1 Å is found in [$Cp^*GaFe(CO)_4$] [145] despite a lesser deviation of the Cp*(centroid)–Ga–Cr vector from linearity.

This behavior is almost analogous to the relationships found between ligand plane angles and interplane distances in the s^0p^0 metallocenes and s^0p^0 Cp′ML_n complexes. In terms of the TSC concept, the symmetric and asymmetric combinations of the π orbitals of the $CO_{equatorial}$ ligands form TSC orbitals (Fig. 20), similarly to the π_{sym} and π_{asym} orbitals of Cp. As we have seen, the driving force for ligand bending is rooted in the additional energy gained from interligand attractions. Calculations show that through-space interaction comes into being if the interplane distance in the linear $Cp^*M_1{-}M_2(CO)_n$ construction is shorter than ca. 4.2–4.3 Å. This correspondence to the Cp–Cp system is reasonable since the same orbitals, viz. p_z of carbon, are involved in TSC of the Cp and CO ligands.

Along these lines it is obvious why the compounds $Cp^*InCr(CO)_5$ and $Cp^*GaCr(CO)_5$ are significantly bent. The numerical values of the Cp*(centroid)–M and M–Cr distances reported [148] would project interplanar distances between Cp* and the $CO_{equatorial}$ groups as long as 4.753 and 4.315 Å, respectively, in a linear arrangement. In this case TSC would be absent, but is regained upon bending. EHMO simulations reveal that, if the distance between the borders of Cp^- and $4 \times CO_{eq}$ groups is 3.8 Å, TSC splitting is ca. 0.1 eV, allowing better overlap of the new bonding TSC orbitals with the metal s,p set. In fact, the border distances between the Cp* plane and the $4CO_{eq}$ plane determined from the

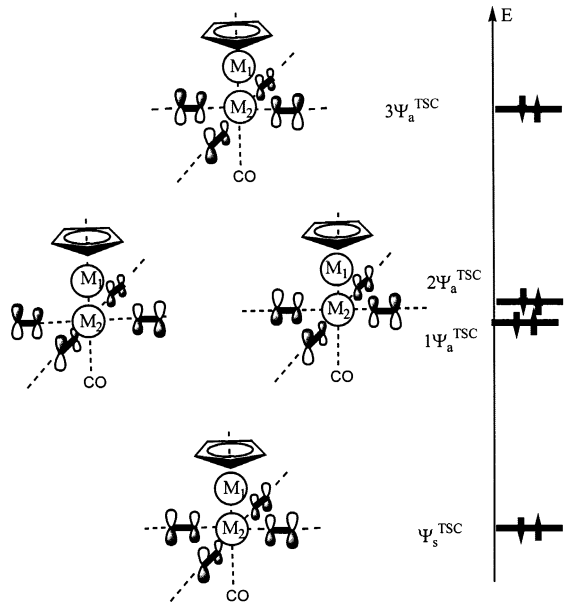

Fig. 20. Splitting of the through space orbitals of four equatorial CO groups in $Cp'M^1–M^2(CO)_5$ complexes.

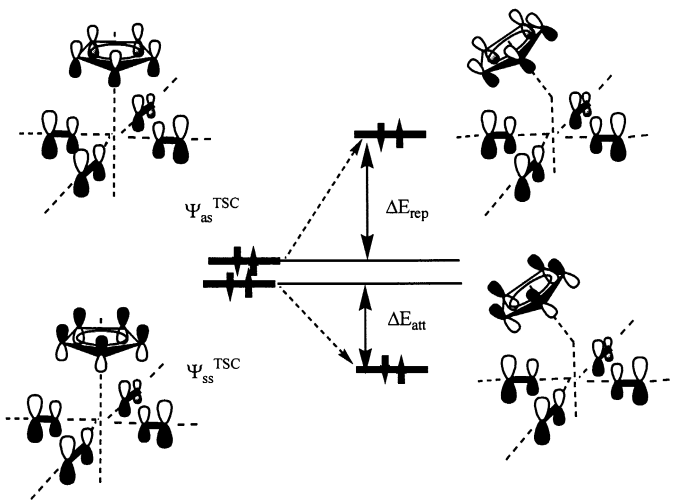

Fig. 21. Change in splitting of the $\Psi_{as}^{TSC}/\Psi_{ss}^{TSC}$ orbitals of four equatorial CO and the Cp unit in linear $Cp'M^1–M^2(CO)_5$ upon bending.

crystallographic data are identical in both cases, viz. 3.84 and 3.83 Å. Fig. 21 shows the splitting of the Ψ_{ss}^{TSC} and Ψ_{as}^{TSC} orbitals, which are constructed from π_{sym} of Cp and the symmetric combination of the four CO π-orbitals. While in the linear arrangement at the left there is no TSC because the interplane distance is too long, bending increases TSC corresponding to vdW repulsion (ΔE_{rep}) and vdW attraction (ΔE_{att}). The former outweighs the latter unless electron density is removed from the high-lying TSC orbital.

On the other hand, if the interplane distance allows TSC between Cp′ and the four CO groups, as in Cp*Ga $Fe(CO)_4$ ($L \sim 4.1$ Å) [145], the linear construction is preferred because of more effective TSC.

3.1.2. σ acceptor properties

In contrasting the acceptor properties of the metal s^0p^0 and s^2p^0 systems, it is essential to implicate the possibility of s,p mixing. From the valence state ionization potentials it is obvious that for the p block elements, unlike the s block analogues, the cost of s,p mixing is rather high to be reasonable. Note that the ($s \rightarrow p$) promotion energies between the two metal blocks differ by several electron volts [152,153]. Consequently, the metal lone pair in [Cp′M:] should be envisioned as being largely s in character with the result that only the δ-symmetric $2e_1$ MO (Figs. 2 and 3), which is anti-bonding and metal-p-like, can function as σ acceptor. Since in addition the nucleophilic attack at p_z is blocked due to the presence of occupied an s, this attack can occur only coplanar to the Cp ring plane, which is sterically unfavorable, indeed. Similarly, the Cp(centroid)–M–L_n angle in the one, two or three legged structures is nearly rectangular and thus far from linearity.

Ab initio calculations on Cp*GeCl show that a linear (C_{5v}) structure is strained, this strain being reduced when the angle between the Ge-to-ring vector and the Ge–Cl bond is 110° [154]. The authors claim that bending transforms the lone pair orbital to an sp hybrid pointing away from both ligands. Compared to this rehybridization model, the TSC concept offers a more appealing explanation. The molecular structure is distinguished by a short Cp(plane)–metal distance (2.1–2.3 Å) and a similarly short Cp(plane)–Cl distance, suggesting strong interligand vdW repulsion. This is diminished by Cp ring slippage like that sketched for $Cp'AlCl_3$ in Fig. 6. Such a scenario is found in the $\{\eta^3\text{-}CpBiCl_2\}_n$ polymer with a Bi–Cp(plane) distance of 2.31–2.34 Å [155], or in dimeric $(\eta^3\text{-}Cp'BiCl_2)_2$ (Cp′ = 1.2.4-tri-*tert*-butylcyclopentadienyl) with a distance of ca. 2.4 Å [156]. Other examples of the η^3-bonding mode are $Cp^*Ge^{II}Cl$ [157], $Cp^*Ge^{II}Py$, and $Cp^*Sn^{II}Py$ [61], and $[(\eta^3\text{-}CpSn(\mu\text{-}N{=}C(NMe_2)_2)]_2$ [158,159]. In virtually all these cases, the metal–ligand vector tends to lie coplanar to the Cp plane.

The importance of size effects on structure is obvious in the series of Group 15 complexes $Cp'ECl_2$ (E = P, As, Sb, Bi and $Cp' = C_5H(CHMe_2)_4$) [160]. As the element–nearest carbon(Cp′) distance increases in the series (1.86, 2.056, 2.33, 2.46 Å) there is a concomitant gradual increase in hapticity $\eta^1 \rightarrow \eta^3$. On the other hand, the electronic properties of the L_n ligands in $[Cp^*X_2As:]$ (X = F, Br, I) [161], and $[Cp^*Cl(NR^1R^2)As:]$ [162] do not seem to have any noticeable effect on the approximate η^3-Cp* bonding mode. In contrast, if the Bi–Cp′(plane) distance is

increased to about 2.77 Å (cf. with 2.46 Å above) in ($\eta^5Cp^*_2Al$)(η^5-Cp*Bi)(ηAlI_4)(AlI_4) then the hapticity also increases [163]. A quite analogous restoration of the η^5 bonding mode occurs when in dimeric $[\eta^3Cp'BiCl_2]_2$ (Cp′ = 1,2,4-tri-*tert*-butylcyclopentadienyl), the Bi–Cl distance is increased (from 2.6 to 2.9 Å) in going to $[Cp'BiCl^*_2BiCl_3]_2$ without, however, changing the Bi–Cp distance (ca. 2.4 Å) [156].

3.2. s^2p^0 metallocenes

Although being only a weak σ acceptor (see below), the [Cp′M:] species exhibits, similar to the six electron [Cp′M], both π-donor and π-acceptor properties. Even the $CpML_n$ (M = Ge, Sn, Pb) adducts can function as π acceptors, giving additional metal–olefin bonding [164]. Furthermore, the unusual cations $[\eta^5\text{-}Cp_2M_3]^+$ (M = In, Tl) [165] are formed as well as 'zig–zag' chain polymers such as $\{\eta^5\text{-CpIn}\}_\infty$, $\{\eta^5\text{-CpTl}\}_\infty$ [166,167] and linear $\{\eta^5\text{-Cp'Tl}\}_\infty$ ($Cp' = Bz_5C_5$) [168]. Of course, the most famous reaction is that with another Cp′ unit yielding (s^2p^0) metallocenes.

For an adequate treatment of the s^2p^0 metallocenes, it is essential to know where the lone-pair of the metal is housed, either in the metal s or sp hybrid orbital. The typically bent structure of this category of complexes favored the opinion that the lone-pair orbital is a sp hybrid pointing away from both Cp ligands. However, from various lines of inquiry it is more reasonable to conclude as a reasonable approximation for the whole p-block Cp compounds, that the lone-pair has largely s character. Two points have already been made above in connection with the s^2p^0 half-sandwich compounds, viz. that the high valence state promotion energies and the experimental bond angles militate against s,p mixing. Further indications may be summarized as follows.

(i) According to MO calculations, the lone-pair is predominantly 4s in Cp_2Ge [11] and 6s in $[\eta^5Cp^*_2Tl]^-$ [167]. Furthermore, the HOMO energy falls rapidly with increasing Cp–M distance [11]. If an sp^2 hybrid were involved, the opposite effect should be expected, because of the simultaneous increase in the interplane angle the energy level of the lone pair would be raised.

(ii) From He(I) PE spectra of Cp^*_2Ge and Cp^*_2Sn, the high ionization energies associated with the lone-pair are indicative of a pronounced inertness without large p contribution [169]. Likewise, the red-shift of the band assigned to the lone pair in going down the Cp^*_2M series with M = Si, Ge, Sn, Pb is paralleled by the ionization potentials of the metals [17].

(iii) According to ^{119}Sn Mössbauer spectra, the valence electrons in stannocenes are largely confined to the 5s orbital [170].

(iv) The addition of σ donors to $[Cp_2M:]$ yield complexes with overall C_2 symmetry, pointing to nucleophilic addition to the empty metal p_x orbital and thus disproving the involvement of sp or sp^2 orbitals. Examples are Cp'_2BiCl (Cp′ = 1.2.4-tri-*tert*-butyl cyclopentadienyl) [156] and $Cp_2M(tmeda)$ (M = Pb, Sn) [171,172]. The presence of a filled s,p hybrid MO in the former should force the adoption of a tetrahedral construction of two Cp–M and Cl–M vectors with the lone-pair directed towards sp^3. In the latter, the tmeda ligand would have been a σ acceptor.

(v) If the lone-pair were of the sp or sp^2 type, the [Cp_2M:] species should definitely be a σ acceptor. To the contrary, adducts are formed only with the very strong acceptor BF_3 such as in {$C_6H_4(CH_2C_5H_4)_2Sn \rightarrow BF_3$} [170] and {$Cp_2Sn \rightarrow BF_3$} [173], but even these are very labile [174]. In addition, the ^{119}Sn Mössbauer resonances for Cp_2Sn and $Cp_2Sn(BF_3)$ are very similar, indicating that the lone-pair from the tin nucleus is preserved [173].

With the s character of the lone-pair given, the differences between the s^0p^0 and s^2p^0 metallocenes may be delineated from Fig. 8. There is thus one important difference between the two cases in that for s^2p^0 the anti-bonding a_{1g}^* orbital is occupied and destabilizes the (bonding) $\langle \Psi_{ss}^{TSC} \mid s \rangle$ interaction. Consequently, the bonding in [Cp'_2M:] is realized by six electrons only, instead of eight, participating in the σ-interaction $\langle p_z \mid a_{2u} \rangle$ and two π-interactions $\langle p_x, p_y \mid e_{1u} \rangle$. The destabilization of the Cp–M bond is reflected by a more significant Cp–M bond lengthening accompanying the [Cp′M:] → [Cp'_2M:] complexation relative to the (s^0p^0) systems. For instance, addition of Cp to cationic [η^5-CpSn]$^+$ increases the Cp–metal distance from 2.14 to 2.41 Å [10], and for neutral eight-electron η^5-CpTl, from 2.54 to 2.90–2.92 Å [167].

As shown above, the classification of s^0p^0 metallocenes into slipped, parallel, and bent can elegantly be based on the M–Cp(plane) distance. In the absence of bulky substituents, parallel Cp planes in η^5-arrangements are found at interplane distances in the range 3.7–4.7 Å. Above and below this range bending and slipping occur, respectively. It is interesting to note that in the s^2p^0 counterpart bending sets in at much shorter interplane distances. Thus, (η^5-Cp*)$_2$Si, having an interplane distance of 4.22 Å, exists in both planar and bent configurations [17]. (This is similar to that found in magnesocene, which, however, is known in the linear configuration only).

That bending occurs at smaller interplane distances is an outcome of the weaker M–Cp bonding. All s^2p^0 metallocenes with larger interplane distances are typically bent. The usual explanation for bending is (i) steric congestion and (ii) strong destabilization of the high-lying lone pair due to insufficient s,p_x mixing [10,11,16,17,22]. Neither suggestion, however, is adequate.

For the steric argument, note that an increase in the size of *rigid* Cp′ substituents fosters the tendency towards a linear arrangement (i.e. smaller interplane angles α). This is seen in the series of compounds (with α in parentheses) Cp_2Sn (46°) [31], Cp_2^*Sn (35.4°) [31], ($^iPr_4C_5H)_2Sn$ (27.8°) [175], and $(C_5Ph_5)_2Sn$ (0°) [31], and also $Pb(C_5Me_4H)_2$ (40.3°), $PbCp_2^*$ (29°), $Pb(C_5Bz_5)_2$ (26.6°), $Pb(C_5Me_4(SiMe_2^tBu))$ (0°) [176,177]. The replacement of Cp′ with the large indenyl system, gives (1,3-$(SiMe_3)_2C_9H_5)_2Pb$, which is close to a planar system (interplane angle 7°), because of the vdW repulsion between the Me groups (nearest-neighbor contact 3.9 Å) [178]. In contrast, flexible substituents that can bend back further from the ring plane, do not impede bending. In fact, the degree of bending in $(C_5Bz_5)_2M$ (M = Ge, Sn, Pb), with α in the range 31–36°, is similar to that in the Cp or Cp* analogues [179]. Note further that the change in the π-ring size by replacement of Cp′ with 1-methylboratabenzene C_5H_5BMe in bis(1-methylboratabenzene) compounds of Ge, Sn and Pb affects appreciably neither structure nor properties [180].

Concerning the electronic argument of bending, ab initio calculations suggest very small energy differences between planar and bent conformations. Pertinent values are 0.4 kJ mol^{-1} for Cp^*_2Si and 0.8 kJ mol^{-1} for Cp_2Si [26], although individual numbers vary with the level of theory. Thus a value of 36.8 kJ mol^{-1} for Cp_2Si has also been suggested [181]. Anyway, the isomerization energy is small enough so that both conformations of Cp^*_2Si coexist in the crystal [17,182]. Further data are available for Cp_2Sn (17.1 kJ mol^{-1}) and Cp_2Pb (2.9 kJ mol^{-1}) [128]. In light of these findings, the high-lying lone pair is actually not a major reason for bending.

Clearly, the molecular reason for bending is the same for both classes of metallocenes. The increase in the metal radius and, accordingly, the interplane distance reduces the through-space interaction between the Cp planes, which is compensated by drawing the Cp π-orbital borders together (Fig. 13). In accordance with the splitting of the TSC orbitals of the Cp groups, the bending increases gradually as the interplane distance exceeds ca. 4 Å. This is exemplified by the neutral Cp^*_2E (E = Si, Ge, Sn, Pb) complexes exhibiting Cp–E distances of 2.11 (2.13), 2.21, 2.39, 2.48 Å and interplane angles of 0 (25.3), 22.4, 23, 36 and 43° [17]. (The values in parentheses pertain to bent Cp^*_2Si). Other examples are cationic $[Cp^*_2As]^+$ with distance 2.14 Å and angle 36.5° or in the anionic $[Cp_2Tl]^-$ [167] with distance 2.72 Å and angle 23.3°; in the neutral polymeric links Cp–M–Cp (M = Tl, In) or oligomeric $\{CpM\}_3$ [165] with distances 2.72, 2.7 or 2.85 Å, the angles are 23.3, 52 and 70°.

The difference to the s^0p^0 metallocenes is just the larger sensitivity of these changes as a consequence of M–Cp bond weakening. For the same reason, the tendency to reduced hapticities is more pronounced in the bent s^2p^0 structures, measured by the differences in the C–C bond lengths. Actually in all s^2p^0 bent structures the hapticity is lower than 5, as is already found in bent Cp^*_2Si where the Cp*rings are asymmetrically bonded [17]. Other examples are Cp_2Ge [183], Cp^*_2Ge [10,184], Cp_2Sn [185], Cp^*_2Sn [10], Cp^*_2Pb [185], $[Cp^*_2As][BF_4]$ and $[Cp^*_2Sb][BF_4]$ [186].

The tendency towards a more linear arrangement if bulky rigid substituted Cp′ ligands are introduced results from the vdW repulsion between the substitutents. For example, the complexes Cp'_2M (M = Ge, Sn, Pb; $Cp' = C_5Me_4SiMe'_2Bu$) are planar. But when ^{t}Bu is replaced with Me, rotation about the C(Cp)–Si bond permits bending of the ligand planes [177]. It is worthwhile to emphasize that rotation and bending are similar in energy barrier. As another example, Cp'_2Pb (Cp′ = 1,2,4-tri-isopropylcyclopentadienyl) is planar with 2.47 Å Pb–Cp′ plane distance [187]. If Cp′ = penta-isopropyl cyclopentadienyl is used instead, bending sets in (Pb–Cp′ distance 2.75 Å; interplane angle 170°) [188].

An intriguing situation is encountered if the Cp–M distance falls below that of Cp^*_2Si, where for the s^0p^0 counterparts ring slippage is found. However, slipped sandwich structures are missing for the s^2p^0 metallocenes. The reason is the absence of a free metal s orbital necessary to stabilize M–Cp bonding. What actually might happen structurally if the radius is decreased below that of Si may be seen by the (unknown) carbocene, $(Cp)_2C$. According to quantum chemical calculations,

$(Cp)_2C$ is unstable and would easily rearrange to a carbene-like structure of C_2 symmetry, with a driving force as high as about 210 kJ mol^{-1}. Ultimately, the most stable species will be phenylcyclopentadiene [189]. A case intermediate between silicocene and carbocene could be phosphocenium Cp_2P^+ for which a slipped bent-up structure is predicted [190].

Summed up, the most important consequences of the s character of the lone-pair are its minimal stereochemical activity and M–Cp bond weakening. Therefore, most differences between the s^0p^0 and s^2p^0 metallocenes concern secondary, not principal, variations in the structural and reactivity patterns. We have already noted above that the $[Cp'_2M:]$ complexes have only very weak donor properties towards BF_3, testifying to the poor p character of the lone-pair. Compared to this, the acceptor properties are far more significant.

3.2.1. Acceptor properties

The F orbital (LUMO, Fig. 15) as the anti-bonding part of the $\langle \pi_{asym} \mid p_{x,y} \rangle$ interaction is the main contributor to the acceptor properties of bent (s^2p^0) sandwich complexes. Due to bending of the Cp planes, the anti-bonding orbitals gain more metal-like p character. This is displayed by the bathochromic shift of the electronic absorption of Cp^*_2Si (colorless), Cp^*_2Ge (light yellow), Cp^*_2Sn (orange), and Cp^*_2Pb (red) [17], in line with the increasing Cp–M distance and, consequently, the bending angle. Of course, addition of σ donors destabilizes the bonding between the metal p_x and p_y and the symmetric combination of the π_{asym} Cp orbitals.

From the TSC point of view, coordination of a donor is due to the interaction between the asymmetric combination of the two Cp π_{asym} orbitals and the σ orbital of the donor ligand (or the symmetric part of the donor L_n group orbital) with the metal p_x orbital (Fig. 17). The electron density (two electrons) donated to p_x stems concomitantly from both Cp groups and the L_n system, thereby strengthening the TSC between the ligands. Formally, the coordination of L_n reduces the M–Cp bonding with, finally, the Cp ligand acting as a 2 electron donor. In fact, ab initio calculations testify to the metal mediated displacement of electron density from the L's lone-pair to the Cp rings [171]. This leads to an increase in the M–Cp distance and in turn to the increase in the interplane angle and a lowering in the Cp–M bond hapticity. For example, the complexes Cp_2Pb and Cp_2Sn give the adducts $Cp_2M(tmeda)$ in the η^3 bonding mode. The M–C bonds 2.77–2.817 Å (for Sn) [171] and 2.8–2.9 Å (for Pb) [172] are elongated relative to those observed in the isolated metallocenes (2.56–2.79 Å for Sn and 2.78 Å for Pb). Concomitantly, the Cp–metal–Cp angles change for Cp_2Sn from 144 to 131.4° and for the Pb analog from 138 to 128.8°.

Similarly, addition of Cl^- to $[Cp'_2Bi]^+$ ($Cp' = 1.2.4$-tri-*tert*-butylcyclopentadienyl) gives $[\eta^3\text{-}Cp'_2BiCl]$ [156]. This complex may not be regarded as ionic, but instead as having been formed by nucleophilic addition to the empty anti-bonding F orbital of metal (Fig. 15). This is concluded from the C_2 structure, arguing against s,p mixing, as noted above.

Finally, it should be noted that similarly to the [CpM:] species, the bent [Cp_2M:] complexes are carbene-like, displaying weak electrophilic behavior relative to the non-Cp ligands [10]. Actually, Cp^*_2Si can be regarded as 'a hypercoordinated, nucleophilic substrate', which changes the oxidation state from $+2$ to $+4$, and the hapticity from η^5 to η^1, by π^* attack of CO, CN [191], CO_2, COS, CS_2, and RNCS (R = methyl, phenyl) [192], or aldehydes and ketones [193]. In all these cases the initial reaction step is thought to be formation of a three-membered ring compound, according to the carbene property of Si in Cp^*_2Si.

3.3. Tris(Cp) complexes

We have seen that bending in both s^0p^0 and s^2p^0 metallocenes provokes σ acceptor properties via the anti-bonding F orbital (Fig. 15). The fact that the lone pair in the s^2p^0 species is more core-like, not giving s,p mixed orbitals, permits face-to-face interaction between π-donors and the anti-bonding orbital G (Fig. 15). Since, in addition, all metallocenes can act as π donors, polymeric compounds containing triangular Cp'_3M groups, such as $\{Cp_2Pb\}_\infty$ come into being [194]. The paddle-wheel structure of the [Cp_3M:] link is found in the zig–zag, hexanuclear and sinusoidal, but no linear, polymers.

The nucleophilic addition of Cp anions affords various anionic π-complexes of the general formula $[Cp_{2x+1}M_x]^-$ [128,167,195]. In the case of Sn or Pb anionic ion-contacted π complexes, the η^5-Cp bonding mode is found. For the ion-separated $[Cp_3M]^-$ units (M = Sn, Pb), ab initio MO calculations point to relatively high association energies between Cp^- and [Cp_2M:] (95 and 128 kJ mol^{-1}, respectively). However, the calculated structures deviate noticeably from the experimental ones. First, the calculated Cp(centroid)–M distances are too long (2.72 vs. 2.57 Å for Sn, and 2.76 vs. 2.68 Å for Pb). Second, the calculated η^5-Cp bonding in the paddle-wheel C_{3h} geometry contrasts with the experimental η^3 bonding and distortion towards a pyramidal geometry [128,195].

Fortunately, these discrepancies can be rationalized in terms of the TSC molecular orbital scheme for [Cp_3M:] in Fig. 18. Accordingly, the bonding interactions between the metal p (not s) set and the TSC orbitals (Ψ^{TSC}_{sa} and Ψ^{TSC}_{as}) yield the bonding orbitals 2a and 1e, while the filled 1a and 1a* orbitals merely contribute to vdW repulsion. Clearly, the main contribution to the thermodynamic stability stems from the $\langle \Psi^{TSC}_{sa} \mid p_z \rangle$ interaction, whose effectiveness depends on the energy of Ψ^{TSC}_{sa}. It can be calculated that for the ion-separated $[Cp_3M]^-$ units (M = Sn, Pb) with the Cp–metal distances in the common range 2.5–2.7 Å, the TSC splitting of the π orbitals is only 35–16 kJ mol^{-1}, making the through-space interaction small. An improvement is attained if the splitting between the TSC orbitals can be increased as is the case by slippage of the Cp rings around the metal sphere to each other (toward the z axis, Fig. 19(c)). In the pyramidal construction both the Cp(centroid)–metal–Cp(centroid) angle and the Cp plane border distance are diminished, enhancing the through-space interaction. In other words, the improved $\langle \Psi^{TSC}_{sa} \mid p_z \rangle$ interaction increases the stability of the complex. Compared to this, the other two interactions $\langle \Psi^{TSC}_{as} \mid p_x, p_y \rangle$ (1e) are weak, laying the basis for a gradual change in hapticity $\eta^5 \rightarrow \eta^3$.

Such an enhancement of TSC, however, is not feasible in the $[Cp_3M]^-$ units embedded in polymeric $\{Cp_2Pb\}_\infty$, or in the contact ion complexes $(Cp_2)Sn(\mu\text{-}Cp)Na^*L$ $(L = (Me_2NCH_2CH_2)_2NMe)$ [196], $[Cp_3Sn]^-\cdot[Li(12\text{-crown-}4)_2]^+$, $[Cp_2Pb(\mu\text{-}Cp)Na\cdot(15\text{-crown-}5)]$, $[Cp_5Pb_2]^-[K(2,2,2\text{-crypt})]^+\cdot thf$, $[Cp_2Pb(\mu\text{-}Cp)Pb(\mu\text{-}Cp)Cs(18\text{-crown-}6)]$ and $[Cp_5Pb_2]^-[Li(12\text{-crown-}4)_2]^+\cdot 2thf$ [91], because of their asymmetric construction. Actually, one Cp′ group is about 0.2–0.3 Å farther away from the center than are the other two. In this case the transformation towards a pyramidal structure would solely weaken the $\langle \Psi_{sa}^{TSC} \mid p_z \rangle$ and $\langle \Psi_{as}^{TSC} \mid p_x,\ p_y \rangle$ interactions. Hence the slightly distorted paddle-wheel geometry with η^5-Cp bonding is retained.

The virtually identical geometry of tris-cyclopentadienyl s^0p^0 and s^2p^0 metal systems at Cp′–M distances in the range 2.5–2.8 Å suggests that the $\langle \Psi_{ss}^{TSC} \mid s \rangle$ interaction is not decisive for the trigonal-planar paddle-wheel geometry. From this point of view, the η^5 structure may be adopted, as in Fig. 19, as the common starting point to construct all other varieties of this class. The presence of the s lone pair is discernible only if ligand border–border repulsion comes into play upon increasing either the ligand size or decreasing the Cp′-M distance through smaller metal ions. In the case of the s^0p^0 system, as already shown above, tangential slippage occurs giving stepwise η^3 or even η^1 coordination (Fig. 19(a,b). This geometric modification, however, is unfavorable in the s^2p^0 case because of the destabilizing $\langle \Psi_{ss}^{TSC} \mid s \rangle$ interaction. In this case the paddle wheel structure transforms into the trigonal pyramidal scoop structure (Fig. 19(e)). It is thus the action of the s pair that makes the difference in structure, upon substituting large fluorenyl (Flu) for Cp′, between trigonal planar $[(\eta^1\text{-}Flu)_3Na]^{2-}$ (Fig. 19(b)) with the metal–Cp plane distances maintained at ca. 2.5 Å [131], and trigonal pyramidal $[(\eta^1\text{-}Flu)_3)Sn]^-$ [195] (Fig. 19(e)).

The pyramidal conformation is also adopted by $(\eta^1\text{-}Cp)_3Sb$ [197] and $(\eta^1\text{-}Cp)_3Bi$ [198] with average C–metal bond lengths of 2.25 Å (for Sb) and 2.37 Å (for Bi). The localization of the negative charge of the Cp anion at the Cp border carbon makes the π Cp system reorganize towards a diene structure in the 'red' $(\eta^1\text{-}Cp)_3Bi$, $(\eta^1\text{-}Cp)_3Sb$ or $(\eta^1\text{-}Cp)_3As$ complexes [199]. Evidently, the Cp′ tangential slippage weakens the Cp′–M bonds, mainly lifting the $\langle \Psi_{as}^{TSC} \mid p_x,\ p_y \rangle$ (1e) interaction. In the case of the s^2p^0 systems, ultimately, the stability is based predominantly on one, viz. the $\langle \Psi_{sa}^{TSC} \mid p_z \rangle$, interaction. Therefore the bonding in complexes of Fig. 19(e) is largely of the σ type. The thermochromism of $[Cp_3M:]$ (M = As, Sb, Bi) complexes [199] is arguably due to reversible isomerization of the distorted paddle-wheel and trigonal pyramidal geometries. In fact, according to IR and ^{1}H-NMR spectroscopic data, there is a trend to transforming the π Cp ring and D_{3h} symmetry of the skeleton of 'black' Cp_3Bi into the diene structure of the rings and C_{3v} symmetry for Cp_3As and Cp_3Sb with rapid interconversion of σ- and π bonded rings [199]. Note further that the anti-bonding orbital of the major interaction (2a in Fig. 18), similar to F in Fig. 15, makes the Cp_3M: complex a σ acceptor. This construction, therefore, can react with the Cp′ fragment of another Cp'_3M, forming zig–zag-chain structures as in $(\eta^1\text{-}Cp)_3Bi$ with weak Bi-η^5-Cp (of a neighboring molecule) bonding [198]. In addition to the easy interconversion of σ and π bonded rings, this

propensity opens up good perspectives for applying such complexes as catalysts in organic syntheses [19].

4. Summary and outlook

The TSC concept adds coherence to a field characterized by complexes exhibiting a considerable diversity in molecular structure and properties. It is gratifying how much is accounted for by considering intramolecular attractive and repulsive forces between valence-saturated non-bonded atoms (modified by metal–ligand interaction). Clearly, such forces are operating also with the d metal relatives. The involvement of d orbitals is actually the overriding factor which depletes ligand–ligand repulsion. Thus, the interplane distance in the progenitor ferrocene is smaller than twice the vdW radius of aromatic carbon. The filled high-lying TSC orbital Ψ_{aa}^{TSC} (Fig. 10) contributes largely to the interligand vdW repulsion, unless electron density is withdrawn. This is unavailable for the main group elements, for symmetry reasons, but can be achieved by donating into metal d_{π} orbitals. In this way vdW repulsion partly switches over into vdW attraction, minimizing electron–electron repulsion and allowing the ligands to be drawn more closely to one another. Thus, the parallel ring structure of the d-metal metallocenes is the result of a combined effect of metal d/Cp π orbital overlap and Cp–Cp vdW attraction. Along these lines, the s,p–π, relative to d–π, interactions may not be rendered insignificant. It would indeed be strange to assume that in a formally eighteen electron complex the eight electrons of the s,p set do not become apparent.

Beyond the Cp complexes, the TSC strategy put forward here is of quite general relevance to so-called weak interactions not amenable to a rigorous theoretical treatment, such as agostic interactions, crystal packing effects, non-bonded interactions in vdW complexes, etc. Note, for instance, the 1:1 vdW complex $C_6H_4F_2\cdots NH_3$ (in which the hydrogen atoms are sufficiently far away from the F atoms that hydrogen bonding is absent) [200]. It is intriguing to speculate that a shift in electron density from the high-lying Ψ_{a}^{TSC} to fluorine not only stabilizes the complex but also encourages fluorine to take on another NH_3 molecule. As another example, the well-known fact that the heavier alkaline earth dihalide MX_2 molecules are bent [36,201] is readily explained. Thus, while at long M–X distances there is no interligand TSC interaction in the linear conformation, upon both bending and electron removal from a high-lying anti-bonding TSC orbital, the molecule experiences additional stabilization. In these terms it may be worthwhile to analyze the clustering of water molecules about ions so as to obtain optimal interaction between the TSC orbitals of water and the metal ion AOs. Such studies could add to the theoretical investigations of the structure and reactivity of clusters [202,203] to improve water force field. It has recently been suggested to involve an additional coupling of the intramolecular structure to the electronic environment [204].

A final message from the present paper is that the possibility of charge redistribution converting vdW repulsion into vdW attraction implies that the so-called vdW radius is not a constant, but can vary with the nature of the partner. In this context the various sets of vdW radii and non-bonded radii should be reanalyzed in regard to the molecular environment, since both kinds of radii should be basically equivalent. Even more importantly, the tendency for releasing electron density from high-lying anti-bonding TSC orbitals formed through strong vdW contacts could well be at the roots of the mechanisms of a variety of phenomena including the electric conductivity of graphite, superconducting transitions in organic and inorganic materials, the piezoelectric effect, etc.

References

[1] B. Rhodes, J.C.W. Chien, M.D. Rausch, Organometallics 17 (1998) 1931.
[2] D. Ekeberg, E. Uggerud, Organometallics 18 (1999) 40.
[3] M. Bochmann, D.M. Dawson, Angew. Chem. Int. Ed. Engl. 35 (1996) 2226.
[4] H. Werner, Angew. Chem. Int. Ed. Engl. 22 (1983) 927.
[5] J.M. O'Connor, C.P. Casey, Chem. Rev. 87 (1987) 307.
[6] T.R. Ward, O. Schafer, C. Daul, P. Hofmann, Organometallics 16 (1997) 3207.
[7] P.J. Shapiro, Coord. Chem. Rev. 189 (1999) 1.
[8] P. Hofmann, Angew. Chem. Int. Ed. Engl. 16 (1977) 536.
[9] B.E.R. Schilling, R. Hoffmann, D. Lichtenberger, J. Am. Chem. Soc. 101 (1979) 585.
[10] P. Jutzi, F. Kohl, P. Hofmann, C. Krüger, Y.-H. Tsay, Chem. Ber. 113 (1980) 757.
[11] J. Almloef, L. Fernholt, J.R.K. Faegri, A. Haaland, B.E.R. Schilling, R. Seip, K. Taugboel, Acta Chem. Scand. A 37 (1983) 131.
[12] T.J. Johnson, K. Folting, W.E. Streib, J.D. Martin, J.C. Huffman, S.A. Jackson, O. Eisenstein, K.G. Caulton, Inorg.Chem. 34 (1995) 488.
[13] B.E.R. Schilling, R. Hoffmann, J.W. Faller, J. Am. Chem. Soc. 101 (1979) 592.
[14] C. Gemel, V.N. Sapunov, K. Mereiter, M. Ferencic, R. Schmid, K. Kirchner, Inorg. Chim. Acta 268 (1999) 114.
[15] W. Simanko, W. Tesch, V.N. Sapunov, R. Schmid, K. Kirchner, J. Coddington, S. Wherland, Organometallics 17 (1998) 5674.
[16] M.A. Beswick, J.S. Palmer, D.S. Wright, Chem. Soc. Rev. 27 (1998) 225.
[17] P. Jutzi, U. Holtmann, D. Kanne, C. Krüger, R. Blom, R. Gleiter, I. Hyla-Kryspin, Chem. Ber. 122 (1989) 1629.
[18] J.D. Fisher, P.H.M. Budzelaar, P.J. Shapiro, R.J. Staples, G.P.A. Yap, A.L. Rheingold, Organometallics 16 (1997) 871.
[19] I. Haiduc, F.T. Edelmann, Supramolecular Organometallic Chemistry, Wiley–VCH, New York, 1999, pp. 425–467.
[20] M.A. Paver, C.A. Russell, D.S. Wright, Angew. Chem. Int. Ed. Engl. 34 (1995) 1555.
[21] E.D. Jemmis, P.v.R. Schleyer, J. Am. Chem. Soc. 104 (1982) 4781.
[22] S.G. Baxter, A.H. Cowley, J.G. Lasch, M. Lattman, W.P. Sharum, C.A. Stewart, J. Am. Chem. Soc. 104 (1982) 4064.
[23] S. Harder, Coord. Chem. Rev. 176 (1998) 17.
[24] P. Jutzi, Chem. Zeit 33 (1999) 342.
[25] P. Jutzi, N. Burford, Chem. Rev. 99 (1999) 969.
[26] T.V. Timofeeva, J.H. Lii, N.L. Allinger, J. Am. Chem. Soc. 117 (1995) 7452.
[27] E.A. Robinson, S.A. Johnson, T.-H. Tang, R.J. Gillespie, Inorg. Chem. 36 (1997) 3022.
[28] W.E. Donath, K.S. Pitzer, J. Am. Chem. Soc. 78 (1956) 4562.
[29] L.S. Bartell, J. Chem. Phys. 32 (1960) 827.

[30] M. Schultz, C.J. Burns, D.J. Schwartz, R.A. Andersen, Organometallics 19 (2000) 781.
[31] J.C. Green, Chem. Soc. Rev. 27 (1998) 263.
[32] R.L. DeKock, M.A. Peterson, L.K. Timmer, E.J. Baerends, P. Vernooijs, Polyhedron 9 (1990) 1919.
[33] R.A. Williams, T.P. Hanusa, J.C. Huffman, Organometallics 9 (1990) 1128.
[34] T.K. Hollis, J.K. Burdett, B. Bosnich, Organometallics 12 (1993) 3385.
[35] J.C. Green, D. Hohl, N. Rösch, Organometallics 6 (1987) 712.
[36] M. Guido, G. Gigli, J. Chem. Phys. 65 (1976) 1397.
[37] W.J. Evans, L.A. Hughes, T.P. Hanusa, Organometallics 5 (1986) 1285.
[38] A. Bondi, J. Phys. Chem. 68 (1964) 441.
[39] R.A. Andersen, R. Blom, C.J. Burns, H.V. Volden, J. Organomet. Chem. 312 (1986) C49.
[40] R.A. Andersen, R. Blom, J.M. Bonsella, C.J. Burns, H.V. Volden, Acta Chem. Scand. A 41 (1987) 24.
[41] L. Pauling, The Nature of the Chemical Bond, third ed., Cornell University Press, Ithaca, NY, 1960.
[42] J.M. Robertson, J. Trotter, J. Chem. Soc. (1961) 1115.
[43] R. Hoffmann, A. Imamura, W.J. Hehre, J. Am. Chem. Soc. 90 (1968) 1499.
[44] R. Hoffmann, Acc. Chem. Res. 4 (1971) 1.
[45] M. Ohsaku, H. Murata, A. Imamura, K. Hirao, Tetrahedron 35 (1979) 1595.
[46] I. Lee, Tetrahedron 39 (1983) 2409.
[47] K.K. Baldridge, T.R. Battersby, R.V. Clark, J.S. Siegel, J. Am. Chem. Soc. 119 (1997) 7048.
[48] G. Wolmershaeuser, G. Kraft, Chem. Ber. 123 (1990) 881.
[49] G. Wolmershaeuser, R. Johann, Angew. Chem. Int. Ed. Engl. 28 (1989) 755.
[50] S. Tachiyashiki, H. Yamatera, J. Chem. Soc. Dalton Trans. (1990) 13.
[51] B.E. Fischer, H. Sigel, J. Am. Chem. Soc. 102 (1980) 2998.
[52] M. O'Keeffe, B.G. Hyde, Structure and Bonding in Crystals, vol. 1, Academic Press, New York, 1981, p. 227ff.
[53] V.G. Tsirelson, P.F. Zou, T.-H. Tang, R.F.W. Bader, Acta Crystallogr. Sect. A 51 (1995) 143.
[54] S.C. Sockwell, T.P. Hanusa, Inorg. Chem. 29 (1990) 76.
[55] A.M. Pendás, A. Costales, V. Luana, J. Phys. Chem. B 102 (1998) 6937.
[56] O.M. Cabarcos, C.J. Weinheimer, J.M. Lisy, J. Chem. Phys. 108 (1998) 5151.
[57] O.M. Cabarcos, C.J. Weinheimer, J.M. Lisy, J. Chem. Phys. 110 (1999) 8429.
[58] L. Manceron, L. Andrews, J. Am. Chem. Soc. 110 (1988) 3840.
[59] G.W. Rabe, L.M. Liable-Sands, C.D. Incarvito, K.-C. Lam, A.L. Rheingolg, Inorg. Chem. 38 (1999) 4342.
[60] C. Dohmeier, H. Schnöckel, C. Robl, U Schneider, R. Ahriches, Angew. Chem. Int. Ed. Engl. 32 (1993) 1655.
[61] F.X. Kohl, E. Schlüter, P. Jutzi, C. Krüger, G. Wolmershäuser, P. Hofmann, P. Stauffert, Chem. Ber. 117 (1984) 1178.
[62] S. Harder, M. Lutz, S.J. Obert, Organometallics 18 (1999) 1808.
[63] C. Dohmeier, R. Köppe, C. Robl, H. Schnöckel, J. Organomet. Chem. 487 (1995) 127.
[64] P. Jutzi, A. Seufert, Ang. Chem. 89 (1977) 339.
[65] F.A. Cotton, J. Takats, J. Am. Chem. Soc. 92 (1970) 2353.
[66] R. Goddart, J. Akhtar, K.B. Starowieyski, J. Organomet. Chem. 282 (1985) 149.
[67] Q.T. Anderson, E. Erkizia, R.R. Conry, Organometallics 17 (1998) 4917.
[68] E.D. Jemmis, S. Alexandeatos, P.v.R. Schleyer, A. Streitwieser, F. Schaefer, S. Achayer, J. Am. Chem. Soc. 100 (1978) 5695.
[69] T.C. Bartke, A. Bjorseth, A. Haaland, K.-M. Marstokk, H. Mollendal, J. Organomet. Chem. 85 (1975) 271.
[70] P. Jutzi, E. Schlüter, S. Pohl, W. Saak, Chem. Ber. 118 (1985) 1959.
[71] M.C. Böhm, R. Gleiter, G.L. Morgan, J. Lusztyk, K.B. Starowieyski, J. Organomet. Chem. 194 (1980) 257.
[72] M.F. Lappert, A. Singh, L.M. Engelhardt, A.H. White, J. Organomet. Chem. 262 (1984) 271.
[73] G. Rabe, H.W. Roesky, D. Stalke, F. Pauer, G.M. Sheldrick, J. Organomet. Chem. 403 (1991) 11.

[74] J. Loberth, S.-H. Shin, S. Wocadlo, W. Massa, Angew. Chem. Int. Ed. Engl. 28 (1989) 735.
[75] H. Chen, P. Jutzi, W. Leffers, M.M. Olmstead, P.P. Power, Organometallics 10 (1991) 1282.
[76] R. Faegri, Jr., K. Blom, T. Midtgaard, J. Am. Chem. Soc. 113 (1991) 3230.
[77] P. Jutzi, J. Organomet. Chem. 400 (1990) 1.
[78] L.M. Engelhardt, P.C. Junk, C.L. Raston, A.H. White, J. Chem. Soc. Chem. Commun. (1988) 1500.
[79] W.E. Rhine, G.D. Stucky, J. Am. Chem. Soc. 97 (1975) 737.
[80] P. Margl, K. Schwarz, P.E. Bloechl, J. Chem. Phys. 103 (1995) 683.
[81] P. Margl, K. Schwarz, P.E. Bloechl, J. Am. Chem. Soc. 116 (1994) 11177.
[82] J.D. Fisher, P.J. Shapiro, P.M.H. Budzelaar, R.J. Staples, Inorg. Chem. 37 (1998) 1295.
[83] J.D. Fisher, P.J. Shaoiro, G.P.A. Yap, A.L. Rheingold, Inorg. Chem. 35 (1996) 271.
[84] H.-J. Koch, S. Schilz, H.W. Roesky, M. Noltemeyer, H.-G. Schmidt, A. Heine, R. Herbst-Irmer, D. Stalke, G.M. Sheldrick, Chem. Ber. 125 (1992) 1107.
[85] P.R. Schonberg, R.T. Paine, C.F. Campana, J. Am. Chem. Soc. 101 (1979) 7726.
[86] M. Scherer, T. Kruck, J. Organomet. Chem. 513 (1996) 135.
[87] O.T. Beachley, R.B. Hallock, H.M. Zhang, J.L. Atwood, Organometallics 4 (1985) 1675.
[88] P. Jutzi, B. Krato, M. Hursthouse, A.J. Howes, Chem. Ber. 120 (1987) 565.
[89] A.G. Davies, Organotin Chemistry, VCH, Weinheim, 1977, p. 113.
[90] S. Harder, M.H. Prosenc, U. Rief, Organometallics 15 (1996) 118.
[91] M.A. Beswick, H. Gornitzka, J. Kärcher, M.E.G. Mosquera, J.S. Palmer, P.R. Raithby, C.A. Russell, D. Stalke, A. Steiner, D.S. Wright, Organometallics 18 (1999) 1148.
[92] C. Dohmeir, E. Baum, A. Ecker, R. Köppe, H. Schnöckel, Organometallics 15 (1996) 4702.
[93] R.E. Dinnebier, U. Behrens, F. Olbrich, Organometallics 16 (1997) 3855.
[94] R.E. Dinnebier, F. Olbrich, S. van Smaalen, P.W. Stephens, Acta Crystallogr. Sect. B: Struct. Sci. B 53 (1997) 153.
[95] R.E. Dinnebier, F. Olbrich, G.M. Bendele, Acta Crystallogr. Sect. C: Cryst. Struct. Commun. C53 (1997) 699.
[96] A. Haaland, J. Lusztuk, J. Brunvoll, K.B. Starowieyski, J. Organomet. Chem. 85 (1975) 279.
[97] S. Harder, M.H. Prosenc, Angew. Chem. Int. Ed. Engl. 33 (1994) 1744.
[98] J. Wessel, U. Behrens, E. Lork, R. Mews, Angew. Chem. Int. Ed. Engl. 34 (1995) 2376.
[99] H. Nöth, M. Schmod, Angew. Chem. Int. Ed. Engl. 35 (1996) 292.
[100] K. Faegri, Jr., J. Almloef, H.P. Luethi, J. Organomet. Chem. 249 (1983) 303.
[101] W. Bründer, E. Weiss, J. Organomet. Chem. 92 (1975) 1.
[102] J. Almlöf, K. Faegry, Jr., B.E.R. Schilling, Chem. Phys. Lett. 106 (1984) 266.
[103] T.P. Hanusa, Chem. Rev. 93 (1993) 1023.
[104] R. Gleiter, M.C. Böhm, J. Organomet. Chem. 170 (1979) 285.
[105] J. Lustyk, K.B. Starowieyski, J. Organomet. Chem. 170 (1979) 293.
[106] N.-S. Chiu, F. Schaefer, J. Am. Chem. Soc. 100 (1978) 2604.
[107] A. Almenningen, A. Haaland, J. Organomet. Chem. 170 (1979) 271.
[108] D.J. Burkey, T.P. Hanusa, J. Organomet. Chem. 512 (1996) 165.
[109] P. Jutzi, A. Seufert, J. Organomet. Chem. 161 (1978) C5.
[110] C.T. Burns, D.S. Stelck, P.J. Shapiro, A. Vij, Organometallics 18 (1999) 5432.
[111] C.P. Morley, P. Jutzi, C. Krüger, J.M. Wallis, Organometallics 6 (1987) 1084.
[112] R. Zerger, G. Stucky, J. Organomet. Chem. 80 (1974) 7.
[113] S. Haiti, D. Datta, J. Phys. Chem. 100 (1996) 4828.
[114] J.T. Waber, D.T. Gromer, J. Chem. Phys. 42 (1965) 4116.
[115] R. Blom, K. Faegri, Jr., H.V. Volden, Organometallics 9 (1990) 372.
[116] M. Kaupp, P.v.R. Schleyer, M. Dolg, H. Stoll, J. Am. Chem. Soc. 114 (1992) 8202.
[117] W.J. Evans, L.A. Hughes, T.P. Hanusa, Organometallics 5 (1986) 1285.
[118] T.K. Ghanty, S.K. Ghosh, J. Phys. Chem. 100 (1996) 17429.
[119] M.G. Gardiner, C.L. Raston, C.H. Kennard, Organometallics 10 (1991) 3680.
[120] D. Barr, A.J. Edwards, P.R. Raithby, M.-A. Rennie, K.L. Verhorsvoort, D.S. Wright, J. Organomet. Chem. 493 (1995) 175.

[121] P. Selg, H.H. Brintzinger, R.A. Andersen, I.T. Horvath, Angew. Chem. Int. Ed. Engl. 34 (1995) 791.
[122] C.J. Burns, R.A. Andersen, J. Organomet. Chem. 325 (1987) 31.
[123] R.A. Williams, T.P. Hanusa, J.C. Huffman, J. Chem. Soc. Chem. Commun. (1988) 1045.
[124] D.J. Burkey, R.A. Williams, T.P. Hanusa, Organometallics 12 (1993) 1331.
[125] S. Harder, Angew. Chem. Int. Ed. Engl. 37 (1998) 1239.
[126] S. Harder, M.H. Prosenc, Angew. Chem. Int. Ed. Engl. 35 (1996) 97.
[127] P.S. Tanner, J.S. Overby, M.M. Henein, T.P. Hanusa, Chem. Ber. 130 (1997) 155.
[128] D.A. Armstrong, M.J. Duer, M.G. Davidson, D. Moncrieff, C.A. Russell, C. Stourton, D. Stalke, A. Steiner, D.S. Wright, Organometallics 16 (1997) 3340.
[129] K.F. Purcell, J.C. Kotz, Inorganic Chemistry, Philadelphia, PA, Saunders, 1977, p. 167.
[130] W.J. Evans, K.J. Forrestal, J.W. Ziller, Angew. Chem. Int. Ed. Engl. 36 (1997) 798.
[131] R.E. Dinnebier, S. Neander, U. Behrens, F. Olbrich, Organometallics 18 (1999) 2915.
[132] J.L. Atwood, K.D. Smith, J. Am. Chem. Soc. 95 (1973) 1488.
[133] H. Schumann, S. Nickel, R. Weimann, J. Organomet. Chem. 468 (1994) 43.
[134] O.T. Beachley, Jr., T.D. Getman, R.U. Kirss, R.B. Hallock, W.E. Hunter, J.L. Atwood, Organometallics 4 (1985) 751.
[135] J.S. Poland, D.G. Tuck, J. Organomet. Chem. 42 (1972) 307.
[136] O.T. Bachley, Jr., R. Blom, M.R. Churchill, K. Faegri, Jr., G.C. Fettinger, J.C. Pazik, L. Victoriano, Organometallics 8 (1989) 346.
[137] R.W. Rudolph, D.A. Thompson, Inorg. Chem. 13 (1974) 2779.
[138] A. Haaland, K.-G. Martinsen, S.A. Shlykov, H.V. Volden, C. Dohmeier, H. Schnöckel, Organometallics 14 (1995) 3116.
[139] C. Dohmeier, C. Robl, M. Tacke, H. Schnöckel, Angew. Chem. Int. Ed. Engl. 30 (1991) 564.
[140] D. Loos, H. Schnöckel, J. Gauss, U. Schneider, Angew. Chem. Int. Ed. Engl. 31 (1991) 1362.
[141] C. Callaghan, G.K.B. Clentsmith, G.F.N. Cloke, P.B. Hitchcock, J.F. Nixon, D.M. Vickers, Organometallics 18 (1999) 793.
[142] H. Bürger, E. Baum, H. Schnöckel, A.J. Downs, Angew. Chem. Int. Ed. Engl. 36 (1997) 860.
[143] P. Jutzi, F. Kohl, C. Krüger, Angew. Chem. Int. Ed. Engl. 18 (1979) 59.
[144] P. Jutzi, R. Dickbreder, H. Nöth, Chem. Ber. 122 (1989) 865.
[145] P. Jutzi, B. Neumann, G. Reumann, H.-G. Stammler, Organometallics 17 (1998) 1305.
[146] C. Dohmeier, D. Loos, H. Schnöckel, Angew. Chem. Int. Ed. Engl. 35 (1996) 129.
[147] P. Jutzi, B. Neumann, L.O. Schebaum, A. Stammer, H.-G. Stammler, Organometallics 18 (1999) 4462.
[148] P. Jutzi, B. Neumann, G. Reumann, L.O. Schebaum, H.-G. Stammler, Organometallics 18 (1999) 2550.
[149] A.H. Cowley, V. Lomeli, A. Voigt, J. Am. Chem. Soc. 120 (1998) 6401.
[150] B. Wrackmeyer, Angew. Chem. Int. Ed. Engl. 38 (1999) 771.
[151] J.W. Weiss, D. Stetzkamp, B. Nuder, R.A. Fischer, C. Boehme, G. Frenking, Angew. Chem. Int. Ed. Engl. 36 (1997) 70.
[152] J. Hinze, H.H. Jaffé, J. Phys. Chem. 67 (1963) 1501.
[153] P. Schwerdtfeger, G.A. Heath, M. Dolg, M.A. Bennett, J. Am. Chem. Soc. 114 (1992) 7518.
[154] A. Haaland, B. Schilling, Acta Chem. Scand. A 38 (1984) 217.
[155] W. Frank, J. Organomet. Chem. 386 (1990) 177.
[156] H. Sitzmann, G. Wolmershaeuser, Chem. Ber. 127 (1994) 1335.
[157] L. Fernholt, A. Haaland, P. Jutzi, F.X. Kohl, R. Seip, Acta Chem. Scand. A38 (1984) 211.
[158] D. Stalce, M.A. Paver, D.S. Wright, Angew. Chem. Int. Ed. Engl. 32 (1993) 428.
[159] A.J. Edwards, M.A. Paver, P.R. Raithby, M.-A. Rennie, C.A. Russell, D.S. Wright, J. Chem. Soc. Dalton Trans. (1995) 1587.
[160] Y. Ehleiter, G. Wolmershaeuser, H. Sitzmann, Z. Anorg. Allg. Chem. 662 (1996) 923.
[161] S.E. Avtomonov, K. Megge, S. Wocadlo, J. Lorbereth, J. Organomet. Chem. 524 (1996) 253.
[162] S.E. Avtomonov, K. Megge, X. Li, J. Lorbereth, S. Wocadlo, W. Massa, K. Harms, A.V. Churakov, J.A.K. Howard, J. Organomet. Chem. 544 (1997) 79.
[163] C. Uffing, A. Ecker, E. Baum, H. Schonekel, Z. Anorg. Allg. Chem. 625 (1999) 1354.

[164] F.X. Kohl, R. Dickbreder, P. Jutzi, G. Müller, B. Huber, Chem. Ber. 122 (1989) 871.
[165] A. Dashti-Mommertz, B. Neumüller, S. Melle, D. Haase, W. Uhl, Z. Anorg. Allg. Chem. 625 (1999) 1828.
[166] S. Corbelin, J. Kopf, E. Weiss, Chem. Ber. 108 (1991) 2417.
[167] D.R. Armstrong, R. Herbst-Irmer, A. Kuhn, D. Moncrieff, M.A. Paver, C.A. Russel, D. Stalke, A. Steiner, D.S. Wright, Angew. Chem. Int. Ed. Engl. 32 (1993) 1774.
[168] H. Werner, H. Otto, H.J. Kraus, J. Organomet. Chem. 315 (1986) C57.
[169] G. Bruno, E. Ciliberto, I.L. Fragalà, P. Jutzi, J. Organomet. Chem. 289 (1985) 263.
[170] T.S. Dory, J.J. Zuckerman, J. Organomet. Chem. 264 (1984) 295.
[171] D.R. Armstrong, M.A. Beswick, N.L. Cromhout, C.N. Harmer, D. Monkrieff, C.A. Russell, P.R. Raithby, A. Steiner, A.E.H. Wheatly, D.S. Wright, Organometallics 17 (1998) 3176.
[172] M.A. Beswick, N.L. Cromhout, C.N. Harmer, P.R. Raithby, C.A. Russell, J.S.B. Smith, A. Steiner, D.S. Wright, Chem. Commun. (1996) 1977.
[173] P.G. Harrison, J.J. Zuckerman, J. Am. Chem. Soc. 92 (1970) 2577.
[174] T.S. Dory, J.J. Zuckermann, C.L. Barnes, J. Organomet. Chem. 281 (1985) C1.
[175] D.J. Burkey, T.P. Hanusa, Organometallics 14 (1995) 11.
[176] W.J. Evans, R.D. Clark, K.J. Forrestal, J.W. Ziller, Organometallics 18 (1999) 2401.
[177] S.P. Constantine, H. Cox, P.B. Hitchocj, G.A. Lawless, Organometallics 19 (2000) 317.
[178] J.S. Overby, T.P. Hanusa, P.D. Boyle, Angew. Chem. Int. Ed. Engl. 36 (1997) 2378.
[179] H. Schuman, C. Janiak, E. Hahn, K. Kolax, M.D. Rausch, J.J. Zuckerman, M.J. Heey, Chem. Ber. 119 (1986) 2656.
[180] G.E. Herberich, X. Zheng, J. Rosenplänter, U. Englert, Organometallics 18 (1999) 4747.
[181] T.J. Lee, J.E. Rice, J. Am. Chem. Soc. 111 (1989) 2011.
[182] P. Jutzi, D. Kanne, C. Krüger, Angew. Chem. Int. Ed. Engl. 25 (1986) 164.
[183] M. Grenz, E. Hahn, W.-W. du Moni, J. Pickardt, Angew. Chem. Int. Ed. Engl. 23 (1984) 61.
[184] L. Fernholt, A. Haaland, P. Jutzi, R. Seip, J. Almloef, K. Faegri, Jr., E. Kvale, H. Lütz, B.E.R. Schilling, K. Taugboel, Acta Chem. Scand. A 36 (1982) 93.
[185] J.L. Atwood, W.E. Hunter, J. Chem. Soc. Chem. Commun. (1981) 925.
[186] P. Jutzi, T. Wippermann, C. Krüger, H.-J. Kraus, Angew. Chem. Int. Ed. Engl. 22 (1983) 250.
[187] D.J. Burkey, T.P. Hanusa, J.C. Huffman, Inorg. Chem. 39 (2000) 153.
[188] H. Sitzmann, Z. Anorg. Allg. Chem. 621 (1995) 553.
[189] W.W. Schoeller, O. Friedrich, A. Sundermann, A. Rozhenko, Organometallics 18 (1999) 2099.
[190] T.J. Lee, H.F. Schaefer, III, E.A. Magnusson, J. Am. Chem. Soc. 107 (1985) 7239.
[191] P. Jutzi, D. Eikenberg, B. Neumann, H.-G. Stammler, Organometallics 15 (1996) 3659.
[192] P. Jutzi, D. Eikenberg, A. Möhrke, B. Neumann, H.-G. Stammler, Organometallics 15 (1996) 753.
[193] P. Jutzi, D. Eikenberg, E.-A. Bunte, A. Möhrke, B. Neumann, H.-G. Stammler, Organometallics 15 (1996) 1930.
[194] J.S. Overby, T.P. Hanusa, V.G. Young, Jr., Inorg. Chem. 37 (1998) 163.
[195] A.J. Edwards, M.A. Paver, P.R. Raithby, C.A. Russell, D. Stalke, D.S. Wright J. Chem. Soc. Dalton Trans. (1993) 1465.
[196] M.G. Davidson, D. Stalke, D.S. Wright, Angew. Chem. Int. Ed. Engl. 31 (1992) 1226.
[197] M. Birkhahn, P. Krommes, W. Massa, J. Lorberth, J. Organomet. Chem. 208 (1981) 161.
[198] L. Lorberth, W. Massa, S. Wocadlo, I. Sarraje, S.-H. Shin, X.-W. Li, J. Organomet. Chem. 485 (1995) 149.
[199] B. Deubzer, M. Elian, E.O. Fischer, H.P. Fritz, Chem. Ber. 103 (1970) 799.
[200] Y. Hu, X. Yang, S. Yang, J. Chem. Phys. 111 (1999) 134.
[201] L. Seijo, Z. Barandiarán, J. Chem. Phys. 94 (1991) 3762.
[202] (a) S.E. Rodriguez-Cruz, R.A. Jockusch, E.R. Williams, J. Am. Chem. Soc. 121 (1999), 1986. (b) S.E. Rodriguez-Cruz, R.A. Jockusch, E.R. Williams, J. Am. Chem. Soc. 121 (1999) 8898.
[203] M. Peschke, A.T. Blades, P. Kebarle, J. Phys. Chem. A 102 (1998) 9978.
[204] B. Chen, J. Xing, J.I. Siepmann, J. Phys. Chem. B 104 (2000) 2391.